NAVAL POSTGRADUATE SCHOOL

MONTEREY, CALIFORNIA

THESIS

KILL VEHICLE EFFECTIVENESS FOR BOOST PHASE INTERCEPTION OF BALLISTIC MISSILES

by

Florios Bardanis

June 2004

Thesis Co-Advisor:	Phillip E. Pace
Thesis Co-Advisor:	Murali Tummala

Approved for public release; distribution is unlimited

THIS PAGE INTENTIONALLY LEFT BLANK

REPORT DOCUMENTATION PAGE			Form Approved OMB No. 0704-0188
Public reporting burden for this collection of information is estimated to average 1 hour per response, including the time for reviewing instruction, searching existing data sources, gathering and maintaining the data needed, and completing and reviewing the collection of information. Send comments regarding this burden estimate or any other aspect of this collection of information, including suggestions for reducing this burden, to Washington headquarters Services, Directorate for Information Operations and Reports, 1215 Jefferson Davis Highway, Suite 1204, Arlington, VA 22202-4302, and to the Office of Management and Budget, Paperwork Reduction Project (0704-0188) Washington DC 20503.			
1. AGENCY USE ONLY *(Leave blank)*	**2. REPORT DATE** June 2004	**3. REPORT TYPE AND DATES COVERED** Master's Thesis	
4. TITLE AND SUBTITLE: Kill Vehicle Effectiveness for Boost Phase Interception of Ballistic Missiles			**5. FUNDING NUMBERS**
6. AUTHOR(S) Florios Bardanis			
7. PERFORMING ORGANIZATION NAME(S) AND ADDRESS(ES) Center for Joint Services Electronic Warfare Naval Postgraduate School Monterey, CA 93943-5000			**8. PERFORMING ORGANIZATION REPORT NUMBER**
9. SPONSORING /MONITORING AGENCY NAME(S) AND ADDRESS(ES) N/A			**10. SPONSORING/MONITORING AGENCY REPORT NUMBER**
11. SUPPLEMENTARY NOTES The views expressed in this thesis are those of the author and do not reflect the official policy or position of the Department of Defense or the U.S. Government.			
12a. DISTRIBUTION / AVAILABILITY STATEMENT Approved for public release; distribution is unlimited			**12b. DISTRIBUTION CODE** A

13. ABSTRACT (maximum 200 words)

Boost phase interception of ballistic missiles is envisioned as the primary response of the layered defense architecture implemented in the ballistic missile defense system. A limited time frame in which to take action and the necessity to implement hit-to-kill technology in the kill vehicle counterbalances the many advantages of boost phase interception. Direct hit missile technology is constrained by the requirement to minimize miss distance to a negligible amount between the kill vehicle and optimum aimpoint on the target. This thesis examines kill vehicle effectiveness, which is tantamount to miss distance, as a function of both the kill vehicle maximum acceleration capability and the guidance system time constant necessary to destroy a target. The kill vehicle guidance system is modeled in MATLAB as a fifth-order binomial series with proportional navigation. The simulation examines the effect of an accelerating target attributed to powered flight and aimpoint displacement caused by a shift in tracking point from the target plume to the payload when resolution occurs. The kill vehicle minimum requirements as indicated by the simulation include a lateral acceleration capability of four times the target acceleration and a guidance system time constant that is less than one-tenth the estimated flight time.

14. SUBJECT TERMS Ballistic Missile Defense System, Layered Defense, Boost Phase Interception, Kill Vehicle, Hit-to-Kill, Proportional Navigation, Miss Distance			**15. NUMBER OF PAGES** 69
			16. PRICE CODE
17. SECURITY CLASSIFICATION OF REPORT Unclassified	**18. SECURITY CLASSIFICATION OF THIS PAGE** Unclassified	**19. SECURITY CLASSIFICATION OF ABSTRACT** Unclassified	**20. LIMITATION OF ABSTRACT** UL

NSN 7540-01-280-5500 Standard Form 298 (Rev. 2-89)
Prescribed by ANSI Std. 239-18

THIS PAGE INTENTIONALLY LEFT BLANK

Approved for public release; distribution is unlimited

KILL VEHICLE EFFECTIVENESS FOR BOOST PHASE INTERCEPTION OF BALLISTIC MISSILES

Florios Bardanis
Lieutenant, Canadian Navy
B.Eng., Concordia University, 1989

Submitted in partial fulfillment of the
requirements for the degree of

MASTER OF SCIENCE IN ELECTRICAL ENGINEERING

from the

NAVAL POSTGRADUATE SCHOOL
June 2004

Author: Florios Bardanis

Approved by: Phillip E. Pace
Thesis Co-Advisor

Murali Tummala
Thesis Co-Advisor

John P. Powers
Chairman, Department of Electrical and Computer Engineering

THIS PAGE INTENTIONALLY LEFT BLANK

ABSTRACT

Boost phase interception of ballistic missiles is envisioned as the primary response of the layered defense architecture implemented in the ballistic missile defense system. A limited time frame in which to take action and the necessity to implement hit-to-kill technology in the kill vehicle counterbalances the many advantages of boost phase interception. Direct hit missile technology is constrained by the requirement to minimize miss distance to a negligible amount between the kill vehicle and optimum aimpoint on the target. This thesis examines kill vehicle effectiveness, which is tantamount to miss distance, as a function of both the kill vehicle maximum acceleration capability and the guidance system time constant necessary to destroy a target. The kill vehicle guidance system is modeled in MATLAB as a fifth-order binomial series with proportional navigation. The simulation examines the effect of an accelerating target attributed to powered flight and aimpoint displacement caused by a shift in tracking point from the target plume to the payload when resolution occurs. The kill vehicle minimum requirements as indicated by the simulation include a lateral acceleration capability of four times the target acceleration and a guidance system time constant that is less than one-tenth the estimated flight time.

THIS PAGE INTENTIONALLY LEFT BLANK

TABLE OF CONTENTS

I. INTRODUCTION....1

II. BALLISTIC MISSILE DEFENSE....3
- A. LAYERED DEFENSE....3
- B. BALLISTIC MISSILE TRAJECTORY....4
  - 1. Boost Phase....5
  - 2. Midcourse Phase....6
  - 3. Terminal Phase....7
- C. BOOST PHASE INTERCEPTION....7
  - 1. Advantages of Boost Phase Interception....7
  - 2. Disadvantages of Boost Phase Interception....8

III. KILL VEHICLE TECHNOLOGIES....9
- A. DIRECT HIT WEAPON TECHNOLOGY....9
- B. SENSOR SUITE....13
- C. GUIDANCE....16
  - 1. Ideal Proportional Navigation....16
  - 2. Binomial Series Representation of PN Guidance System Dynamics....18

IV. SIMULATION....23
- A. NUMERICAL METHOD....23
- B. SYSTEM DYNAMICS....24
- C. SYSTEM IMPLEMENTATION IN MATLAB....25
  - 1. Acceleration Saturation....26
  - 2. Aimpoint Displacement....31

V. CONCLUSION....37

APPENDIX A. ALPHA KV-MODEL....39

APPENDIX B. TRANSFER FUNCTION DERIVATION....41

APPENDIX C. GUIDANCE SYSTEM SIMULATION....45

LIST OF REFERENCES....49

INITIAL DISTRIBUTION LIST....51

THIS PAGE INTENTIONALLY LEFT BLANK

LIST OF FIGURES

Figure 1. Layered Defense (After Ref. 2). 4
Figure 2. Ballistic Missile Trajectory (From Ref. 3)....4
Figure 3. Boost Phase Burn Times for IRBM (After Ref. 2). 5
Figure 4. Unopposed Ballistic Missile Flight (From Ref. 5)....7
Figure 5. Target Payload with Optimum Hit-Point (After Ref. 9). 11
Figure 6. Required Kinetic Energy for Optimum Kill Vehicle. 12
Figure 7. Exo-atmospheric Kill Vehicle (From Ref. 5). 13
Figure 8. MWIR/LWIR Band-Ratioing. 15
Figure 9. Dual Band IR Image of Atlas V Launch 21 August 2002 (From Ref. 13). 16
Figure 10. Ideal Representation of Proportional Navigation (After Ref. 17)....17
Figure 11. Fifth-Order Representation of PN Guidance System (After Ref. 18)....19
Figure 12. Comparison of System Dynamics (From Ref. 17). 20
Figure 13. Simulation of Guidance System Components. 25
Figure 14. Normalized KV Acceleration for Zero Lag System. 27
Figure 15. Normalized Miss Distance Due To Target Acceleration for $N' = 3$ 28
Figure 16. Normalized Miss Distance Due To Target Acceleration for $N' = 4$ 29
Figure 17. Normalized Miss Distance Due To Target Acceleration for $N' = 5$ 30
Figure 18. Normalized Acceleration Due To Aimpoint Shift For Ideal System....31
Figure 19. Normalized Miss Distance Due to Aimpoint Displacement for $N' = 3$ 33
Figure 20. Normalized Miss Distance Due to Aimpoint Displacement for $N' = 4$ 34
Figure 21. Normalized Miss Distance Due to Aimpoint Displacement for $N' = 5$ 34
Figure 22. Transfer Function Representation. 41

THIS PAGE INTENTIONALLY LEFT BLANK

LIST OF TABLES

Table 1. Approximate Coordinates at Termination of Boost Phase (After Ref. 2).....6
Table 2. KV Acceleration Requirements for Zero Miss Distance. 30
Table 3. Aimpoint Displacement Results. 35
Table 4. KV Guidance System Time Constants (Seconds). 35

THIS PAGE INTENTIONALLY LEFT BLANK

ACKNOWLEDGMENTS

I greatly appreciate the support provided by Dr. Pace and Dr. Tummala. As a mechanical engineer prior to attending the Naval Postgraduate School, I was under the impression that electrical engineering was really black magic. Thanks to the outstanding teaching skills of all the staff in the Electrical and Computer Engineering Department, I have acquired the necessary knowledge to become a more effective combat systems engineer. I would also like to express my sincere gratitude to all the staff at the Dudley Knox Library. They always responded to my requests for information in a very timely manner.

THIS PAGE INTENTIONALLY LEFT BLANK

EXECUTIVE SUMMARY

The United States Department of Defense is developing a ballistic missile defense system to provide a layered defense capability for national and theater level protection. Boost phase interception of ballistic missile threats is envisioned as the primary response of the layered defense network. Currently operational weapon systems can engage ballistic missile threats in the later stages of their flight; however, there is a lack of fielded systems for boost phase interception.

A limited time frame in which to take action and the necessity to implement hit-to-kill technology in the kill vehicle counterbalances the many advantages of boost phase interception. Direct hit missile technology is constrained by the requirement to minimize miss distance to a negligible amount between the kill vehicle and optimum aimpoint on the target payload. This thesis examines kill vehicle effectiveness, which is tantamount to miss distance, as a function of both the kill vehicle maximum acceleration capability and the guidance system time constant necessary to destroy a given target. All results promulgated in this document are based on simulated engagements between a threat ballistic missile and a kill vehicle employing proportional navigation guidance.

The kill vehicle minimum requirements include a lateral acceleration capability of four times the target acceleration and a guidance system time constant that is less than one-tenth the estimated flight time after warhead resolution. Development of a kill vehicle that fulfills these requirements is one step towards the successful implementation of a weapon system that can be utilized to destroy a ballistic missile during the boost phase of its flight.

THIS PAGE INTENTIONALLY LEFT BLANK

I. INTRODUCTION

The United States Department of Defense is developing an integrated ballistic missile defense system (BMDS) to provide national and theater level protection from ballistic missile attacks. BMDS will incorporate layered defense architecture to engage threat missiles at the earliest opportunity. Failure to eliminate a threat will initiate additional engagements by different weapon systems until a positive kill assessment is made. Currently, there are fielded weapon systems that can engage a ballistic missile during the later stages of its flight; however, there are no operational systems that can engage a threat missile during the initial stage of its flight, known as boost phase.

Various weapon systems have been proposed for boost phase interception (BPI) of ballistic missiles, including airborne lasers, space-based intercept missiles, and ground-based intercept missiles. These systems will have different capabilities and limitations and shall require advanced technologies to implement.

This thesis is applicable to ground-based intercept missiles and, in particular, examines the requirements for kill vehicle effectiveness during boost phase interception of ballistic missiles. The kill vehicle is the payload on the intercept missile and may be considered an armored fist, which imparts a destructive force on the threat missile. Kill vehicle effectiveness is gauged by the amount of miss distance at termination of the engagement. Successful boost phase interception is tantamount to complete destruction of the target and necessitates a negligible miss distance from the optimum aimpoint on the target warhead. The kill vehicle incorporates a guidance system to reduce the miss distance to an amount suitable for complete destruction of target. During the boost phase, a target ballistic missile is characterized by a monotonically increasing acceleration rate attributed to powered flight and a brilliant exhaust plume. The effect of target acceleration on miss distance is analyzed during the terminal maneuvers of the kill vehicle, to determine the maximum acceleration requirement for a kill vehicle to impact a specific target. Additionally, the effect of aimpoint displacement associated with transferring the guidance aimpoint from plume to warhead, at such time as resolution occurs, is examined. This analysis leads to determination of a guidance system time constant, which tol-

erates an aimpoint shift while realizing a negligible miss distance at termination of engagement. The analysis is based on a MATLAB simulation of the kill vehicle guidance system, which incorporates a fifth-order binomial series representation of the system dynamics and proportional navigation for the guidance law.

In Chapter II, the thesis commences with a review of layered defense and its applicability to BMDS. Integral to the layered defense scheme are the different phases of a ballistic missile's flight trajectory; consequently, they are defined in this chapter. The final section identifies the advantages and disadvantages of boost phase interception.

Chapter III provides a description of various technologies, which must be developed or further refined in order to deploy an operational kill vehicle for boost phase interception of ballistic missiles. Direct hit weapons technology is identified as the necessary means of conveying a destructive force in the BPI scenario. Furthermore, sensors will play an indispensable role in the successful employment of any weapon system intended for this application. A possible configuration for the kill vehicle sensor suite is provided in this section. Lastly, the main thrust of the thesis revolves around the guidance system utilized in the kill vehicle; therefore, various guidance techniques are identified, and it is reasoned why only proportional navigation was considered suitable for this application. A review of ideal proportional navigation is presented here for comparison purposes. The chapter concludes with a description of a more realistic model for a proportional navigation guidance system, which utilizes a fifth-order binomial series representation for the system dynamics and is employed in the ensuing simulation.

Chapter IV encompasses the simulation. The Runge-Kutta numerical technique is identified as the means of approximating the differential equations that make-up the model. Subsequently, the system dynamics of the model are described. The binomial series representation of the system dynamics is further reduced into components identified in the MATLAB simulation. The results are sub-categorized in sections for acceleration saturation and aimpoint displacement.

The concluding chapter summarizes the results. The Appendices include a listing of the MATLAB code used in the simulation, and a derivation of the seeker transfer function used in the guidance simulation.

II. BALLISTIC MISSILE DEFENSE

Prior to January 2002, the United States missile defense program was organized within two frameworks, national missile defense (NMD) and theater missile defense. The former was intended to protect the continental United States from attacks by inter-continental ballistic missiles (ICBM) while the latter was intended to protect US military forces deployed overseas against all missile attacks, up to and including intermediate range ballistic missiles (IRBM).

In January 2002, the Secretary of Defense ordered the establishment of a single integrated program to develop a ballistic missile defense system capable of defending the United States, its deployed forces, and allies [1]. BMDS shall implement a layered defense battle doctrine, capable of intercepting ballistic missiles in all phases of their flight trajectory. This chapter will describe the principle of layered defense and its application to ballistic missile defense.

A. LAYERED DEFENSE

The principle of layered defense has various interpretations; it is instructive to first examine the naval combat version, which is a precursor to the model utilized by the Missile Defense Agency (MDA). In naval operations, threat evaluation and weapons assignment is based on range, bearing, and range rate of the target to the defending unit. If a positive kill assessment is not made after the primary engagement, the defending unit progressively assigns different weapons systems for target engagement, based on the range from the defending asset to the target. The Missile Defense Agency has juxtaposed this concept with the different segments of a ballistic missile's flight trajectory. The layered defense scheme put forth by MDA [2] includes the following segments in sequential order:

- Boost Segment;
- Midcourse Segment; and
- Terminal Segment.

Each phase of the missile's trajectory is associated with a specific altitude sector above the earth's surface, as depicted in Figure 1. MDA intends to engage and destroy

the threat missile at the earliest possible opportunity; however, if this is unsuccessful, a handover will be made to the next weapon system in the layered defense chain.

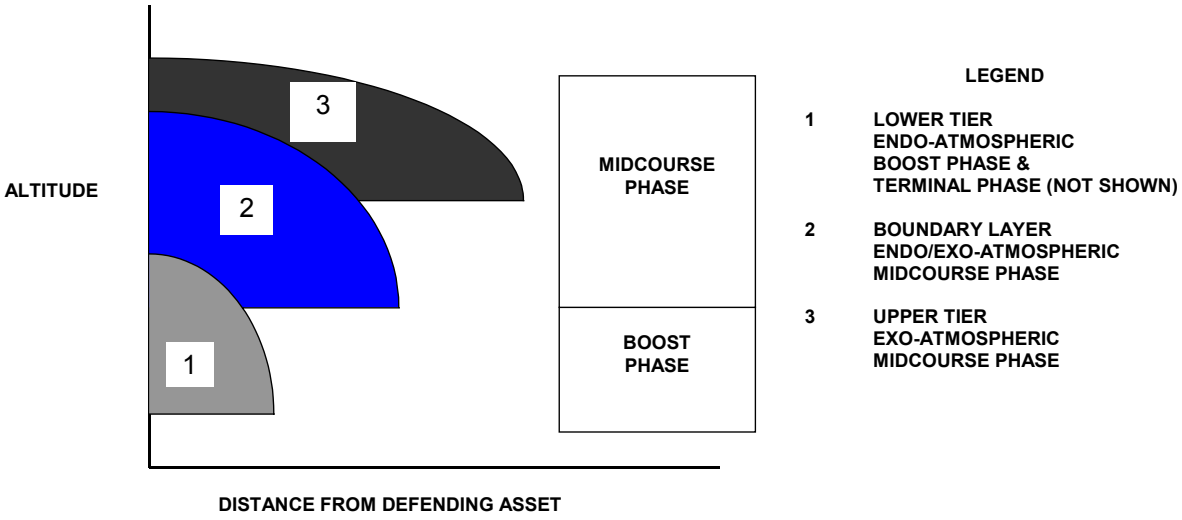

Figure 1. Layered Defense (After Ref. 2).

B. BALLISTIC MISSILE TRAJECTORY

A ballistic missile trajectory is comprised of the following phases: boost phase, midcourse phase, and terminal phase as shown in Figure 2. Each of these phases is further discussed in the following subsections.

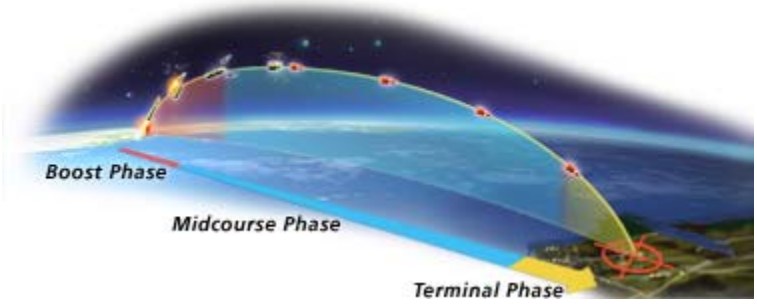

Figure 2. Ballistic Missile Trajectory (From Ref. 3).

1. Boost Phase

The boost phase is initiated with rocket ignition just prior to liftoff and completed after burnout of the final stage of the ballistic missile. During this time frame, the ballistic missile accelerates to its maximum speed. The missile velocity is relatively slow during this phase because the initial velocity is zero and the rocket engine's propulsive force is opposed by the earth's gravity. The discharge of hot propellant gasses makes the exhaust plume highly visible to infrared detectors at great ranges. Thrust is terminated at the end of boost phase.

The duration of boost phase is dependent on the propellant burn rate, the missile range capability, and the average acceleration as shown in Figure 3. The line graph attributed to an acceleration of 3g is indicative of older missile types, such as the SCUD, No Dong 1 (ND-1), and the Chinese Surface-to-Surface Missile 2 (CSS-2); whereas newer missiles have an average acceleration of approximately 10g.

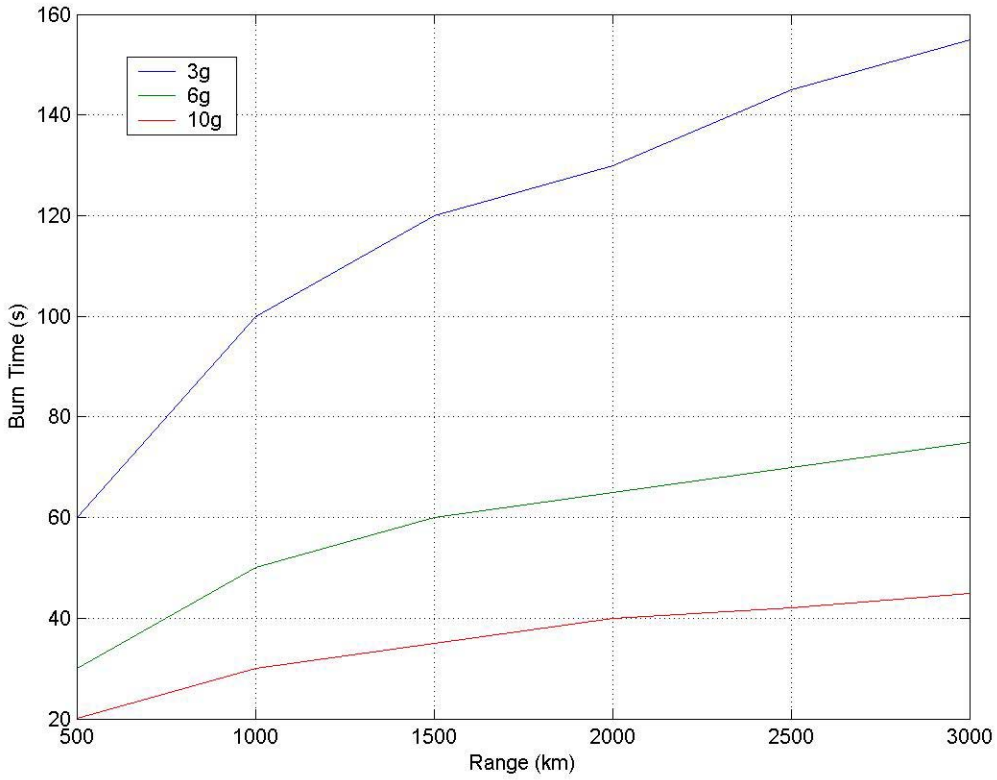

Figure 3. Boost Phase Burn Times for IRBM (After Ref. 2).

Intercontinental ballistic missiles have a range capability in excess of 5000 kilometers and boost phase duration of approximately 240 seconds for rocket engines using liquid propellant and 180 seconds for solid propellant rocket engines [4].

ICBMs will exit the earth's atmosphere by the end of boost phase whereas intermediate range ballistic missiles only reach the periphery of the exo-atmosphere. The maximum altitude and downrange attained by the end of boost phase is dependent on various design parameters including the guidance law utilized, propellant burn rate, acceleration, and launch angle. Typical values are listed in Table 1.

Missile Range (km)	Burnout Altitude (km)	Burnout Range (km)
500	20-40	25-75
1,000	45-70	40-100
2,000	70-130	75-150
3,000	100-170	125-250
10,000	175-220	425-475

Table 1. Approximate Coordinates at Termination of Boost Phase (After Ref. 2).

2. Midcourse Phase

The midcourse phase commences after termination of the boost phase and encompasses the longest segment of the trajectory, approximately 20 to 30 minutes for an ICBM [3]. The weapon payload, which may be a unitary warhead, multiple re-entry vehicles, or submunitions, is deployed during this phase and follows an unpowered ballistic trajectory towards the intended target. The midcourse trajectory will take place in the exo-atmosphere for ICBMs and intermediate range ballistic missiles.

Intercepting the weapon payload during the midcourse phase is complicated by the need to eliminate all submunitions or re-entry vehicles (RV), plus discriminating and excluding any countermeasures and booster debris. Figure 4 provides a pictorial representation of the crowded scenario encountered during the midcourse phase; also shown is

the attitude control module (ACM), which corrects small guidance errors and ensures the weapon maintains the desired course.

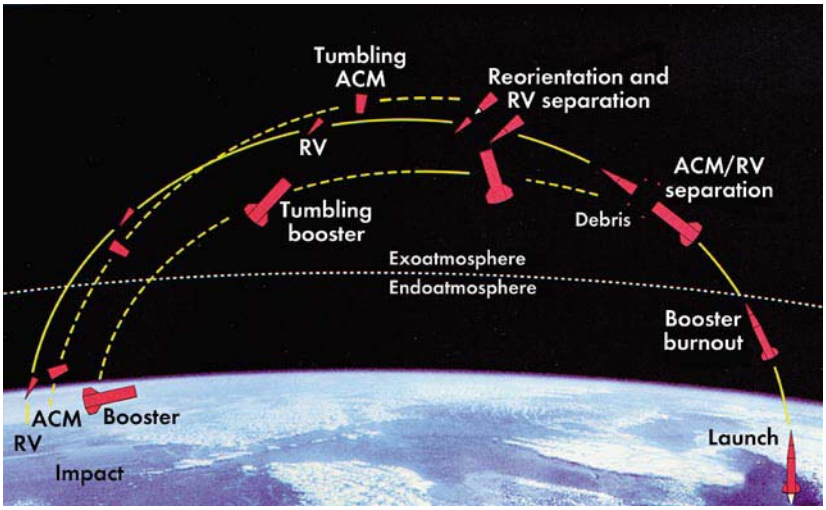

Figure 4. Unopposed Ballistic Missile Flight (From Ref. 5).

3. Terminal Phase

The terminal phase is the ending segment of the missile's flight trajectory. The weapon payload has amassed great speed by the start of this phase; however, re-entry into the earth's atmosphere will impart changes to the weapon's velocity and trajectory. Atmospheric drag will ensure the weapon is separated from the debris field. Lastly, the weapon is capable of maneuvering to avoid interception during this phase.

C. BOOST PHASE INTERCEPTION

Boost phase interception of a ballistic missile threat shall be the primary response of the BMDS layered defense architecture. Boost phase interception has many advantages and disadvantages, identified in the following subsections [6].

1. Advantages of Boost Phase Interception

The advantages of a response in this segment of the layered defense scenario include the following:

- Single target engagement preempts deployment of multiple re-entry vehicles or submunitions from threat missile payload;
- Large infrared signature attributed to the exhaust plume makes ballistic missile readily detectable at long ranges;
- Low velocity of threat missile at commencement of boost phase permits employment of terrestrial interceptor;

- Forward defense presents opportunity to destroy ballistic missile far away from the United States;
- Sensors utilized for BPI will serve as an early warning mechanism for the additional defensive layers; and
- Any ballistic missiles that penetrate this outer layer will be identified for handover and weapons assignment to the inner layers of the defense network.

2. Disadvantages of Boost Phase Interception

Boost phase interception is constrained by the following:

- Limited time span in which to engage target necessitates development of advanced weapons systems to accomplish this mission;
- A ground-based intercept system must be located relatively close to launch point of threat missile;
- The variable acceleration rate attributed to fuel consumption and discarding of spent stages complicates targeting;
- BMDS sensors cannot pre-determine total pitch/rotation the missile must undergo to attain ballistic trajectory;
- Advanced ballistic missiles can maneuver for energy management or intercept avoidance;
- Debris from the engagement, including undestroyed submunitions, may fall on friendly territory; and
- The kill vehicle (KV) must incorporate advanced hit-to-kill technology to ensure complete destruction of the target, including all submunitions.

The development of an effective kill vehicle for boost phase interception is a major undertaking, which necessitates the integration of sensors, lethality enhancement mechanisms, and guidance and control systems in a payload that is deployable from an interceptor missile. A description of these technologies is provided next in Chapter III.

III. KILL VEHICLE TECHNOLOGIES

During the Cold War era, missile interceptors armed with conventional explosive warheads were deemed ineffective at countering ballistic missile threats. Consequently, the United States and the former Soviet Union developed nuclear armed interceptors for employment as anti-ballistic missiles [7]. This solution was politically unacceptable since a nuclear explosion at high altitudes over a defended country would incapacitate numerous electrical and electronic systems in that country. The current solution is implementation of direct hit or hit-to-kill technology, whereby the impact of collision is sufficient to destroy the target. The primary impediment of this technology is the requirement for infinitesimal miss distance between the kill vehicle and optimum aimpoint on the target warhead, to ensure destruction of all submunitions [8]. This chapter considers direct hit weapons technology, the sensor suite, and guidance system requirements for a kill vehicle suitable for boost phase interception.

A. DIRECT HIT WEAPON TECHNOLOGY

The destructive force conveyed by a direct hit weapon is several orders of magnitude greater than a conventional blast fragmentation warhead.

> This focused direct hit impact energy is created by a nearly solid concentration of directed energy, but must rely on the radial expansion of that energy to damage any submunitions not located on the impacting missile flight path [8].

A major constraint of direct hit weapons is locating the aimpoint on the target payload where the maximum number of submunitions will be destroyed. This optimum aimpoint is euphemistically known as the sweet spot. The lethality of a direct hit weapon will deteriorate significantly as the aimpoint is displaced from the sweet spot. This is attributed to decreased radial energy imparted to the area offset from the aimpoint.

The ALPHA-KV analytical model developed by Orphal [9] graphically illustrates that aimpoint errors necessitate increased kinetic energy for the kill vehicle to achieve lethality. The model assumes that the crater volume ν_C, caused by the kill vehicle collision with the target, is proportional to the impact kinetic energy

$$v_C = \frac{\alpha m V^2}{2} \tag{1}$$

where m is the kill vehicle mass and V is the closing velocity. The proportionality constant α (cm^3/J) is determined experimentally or by using a cratering model such as the Tate model [10]. The Tate theory of penetration states that α can be approximated by the relationship

$$\alpha \approx \frac{4\sqrt{\frac{\rho_T}{\rho_{KV}}}}{R_T\left(1+\sqrt{\frac{\rho_T}{\rho_{KV}}}\right)^2} \tag{2}$$

where ρ_T and ρ_{KV} are the bulk densities of the target and kill vehicle, respectively. The parameter R_T (N/cm^2) is determined from the sound speed of the target c_o and the Brinell hardness number (BHN) of the target in

$$R_T = 4.2\text{x}10^7\,\text{BHN}\left[\frac{2}{3}+\ln\left(\frac{0.571\rho_T c_o^2}{4.2\text{x}10^7}\right)\right]. \tag{3}$$

The required crater volume is assumed cylindrical and is given by

$$v_C \geq \pi L_C\left(R_o + R_m\right) \tag{4}$$

where L_C is the crater depth, R_o is the minimum crater radius to overlap all submunitions, and R_m is any offset from the optimum, as illustrated in Figure 5 where the submunitions are highlighted in gray. For maximum effectiveness, which is tantamount to zero miss distance, the optimum hit-point would be the geometric center of the payload. If the hit-point is offset by an amount R_m from the optimum location the crater radius will have to be increased to an amount equivalent to $R_o + R_m$.

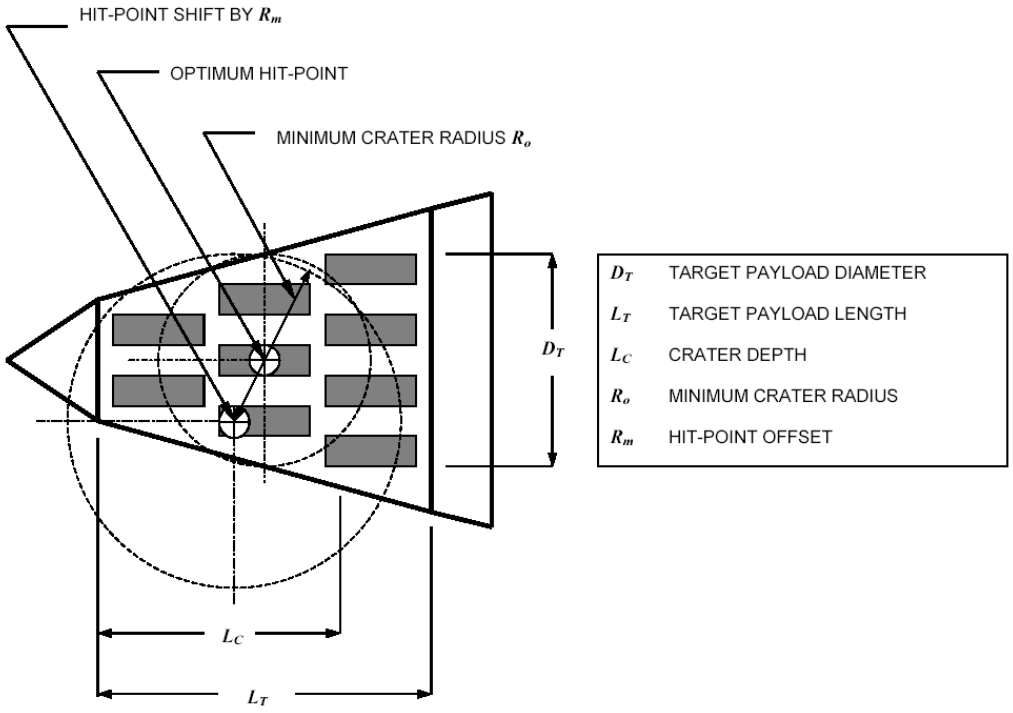

Figure 5. Target Payload with Optimum Hit-Point (After Ref. 9).

Incorporating target parameters in the model calculations, including number of submunition tiers, diameter of individual submunitions, and overall length and diameter of target, optimizes the ALPHA-KV model. The model is easily programmed in MATLAB, attached as Appendix A, and is used to generate Figure 6 which illustrates that the kinetic energy $\left(mV^2/2\right)$ required by the kill vehicle is near linearly proportional to the amount of offset $\left(R_m\right)$ from the sweet spot.

The exact location of the sweet spot is unique to each missile type depending on the payload and geometry and cannot be ascertained precisely with current sensing systems; therefore, a default location must be utilized. This default location must be suitable for all threats, which the direct hit weapon is designed to engage and destroy. Location of the sweet spot is not as critical with respect to targeting unitary warheads.

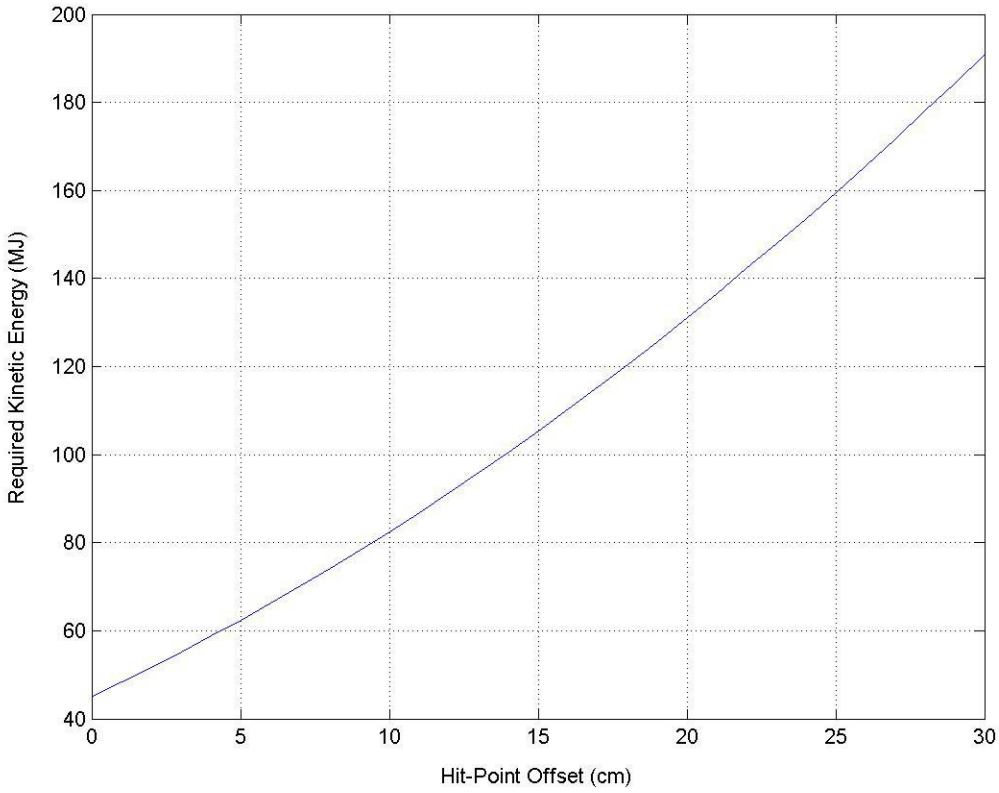

Figure 6. Required Kinetic Energy for Optimum Kill Vehicle.

Kill vehicles for boost phase interception have not been fully implemented to date; however, similar systems for ground-based midcourse defense have been designed and tested. Raytheon has developed and successfully trialed the exo-atmospheric kill vehicle (EKV) pictured in Figure 7. Visible in this schematic representation are two of four thrusters arranged in a cruciform configuration and used to maneuver the KV on the horizontal (pitch) axis and vertical (yaw) axis. The thrusters are part of the divert and attitude control system (DACS) which steers the kill vehicle in accordance with the guidance commands. Most of the forward momentum required by this kill vehicle is provided by the intercept booster's burnout velocity. The kill vehicle weighs approximately 140 pounds and has a length of 55 inches and a diameter of 24 inches [3]. Also identifiable in the left foreground of Figure 7 is the acquisition telescope. The sensor system incorporates three separate sensors, not shown in Figure 7, which measure visible light, mid-wave infrared, and long-wave infrared radiation.

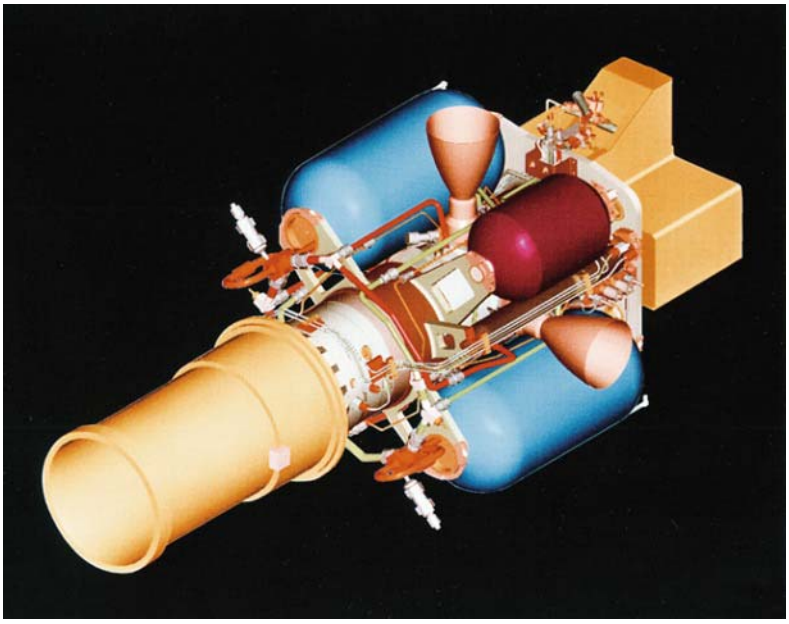

Figure 7. Exo-atmospheric Kill Vehicle (From Ref. 5).

B. SENSOR SUITE

The principal signature of a ballistic missile during its boost phase trajectory is attributed to the exhaust plume. It is characterized by strong emissions in the mid-wave infrared (MWIR) spectrum, 3 to 5 μm, and weaker emissions in the ultraviolet spectrum [11]. Another valuable source of radiation is skin friction from the missile hardbody, which radiates strongly in the long-wave infrared (LWIR) band, 8 to 12 μm.

Launch detection and tracking of a ballistic missile threat will be conducted by a space based infrared (IR) system, which will sense the target exhaust plume and provide a two-dimensional angular measurement of bearing and elevation. Ground-based air defense radars will acquire and track the target after it climbs above the radar horizon. They will provide a three dimensional measurement of target range, bearing, and elevation. The two data types, infrared and radio frequency, will be fused into one threat track and passed to the Battle Management/Command, Control, and Communications (BM/C^3) system for engagement authority [12]. If permission to engage is granted, the target will be designated for weapons assignment. A ground-based intercept (GBI) missile will consequently be launched at the threat missile. Various proposals for intercept launchers

have been made; however, this study will only examine ground-based interceptors. It is assumed that the interceptor will incorporate a global positioning system (GPS) aided inertial navigation system, and communication link with the BM/C^3 system. Initially, the interceptor will guide to the planned intercept point (PIP) generated from the fused data. It will receive target updates on a continuous basis until the kill vehicle is deployed, and its onboard sensors takeover the sensing mission.

The sensor suite onboard the kill vehicle should include a dual-band imaging seeker, operating in the MWIR and LWIR bands. It is implemented with two co-registered quantum-well infrared photodetector (QWIP) focal plane arrays (FPA) [13]. The advantage of this dual-band IR camera is simultaneous imaging of the rocket plume and missile hardbody. Digital image processing (DIP) is required for comparison of the simultaneous MWIR and LWIR images. The DIP algorithm is known as MWIR/LWIR band-ratioing. A plot of the in-band radiance arriving at the MWIR detector versus that of the LWIR detector will generate a line, with a slope equivalent to the ratio between the two bands. Planck's blackbody radiance function is first evaluated as a precursor to determining the band ratio. The radiance function is given by [14]

$$B_\lambda(T) = \frac{2hc^2}{\lambda^5\left[\exp\left(hc/\lambda kT\right)-1\right]} \tag{5}$$

where h is Planck's constant, c is the speed of light, k is Boltzmann's constant, λ is wavelength, and T is temperature. The in-band radiance incident on the sensor optics is then determined by integration of Planck's blackbody radiance function with respect to the wavelengths of interest. The ratio can be evaluated by

$$Ratio = \frac{\int_{MWIR} B_\lambda(T)\,d\lambda}{\int_{LWIR} B_\lambda(T)\,d\lambda}. \tag{6}$$

A proof of concept for dual-band ratioing was developed in MATLAB and is available from the thesis advisor. The model evaluates Equations (5) and (6) and is used to plot the numerator versus denominator of the *Ratio* as shown in Figure 8.

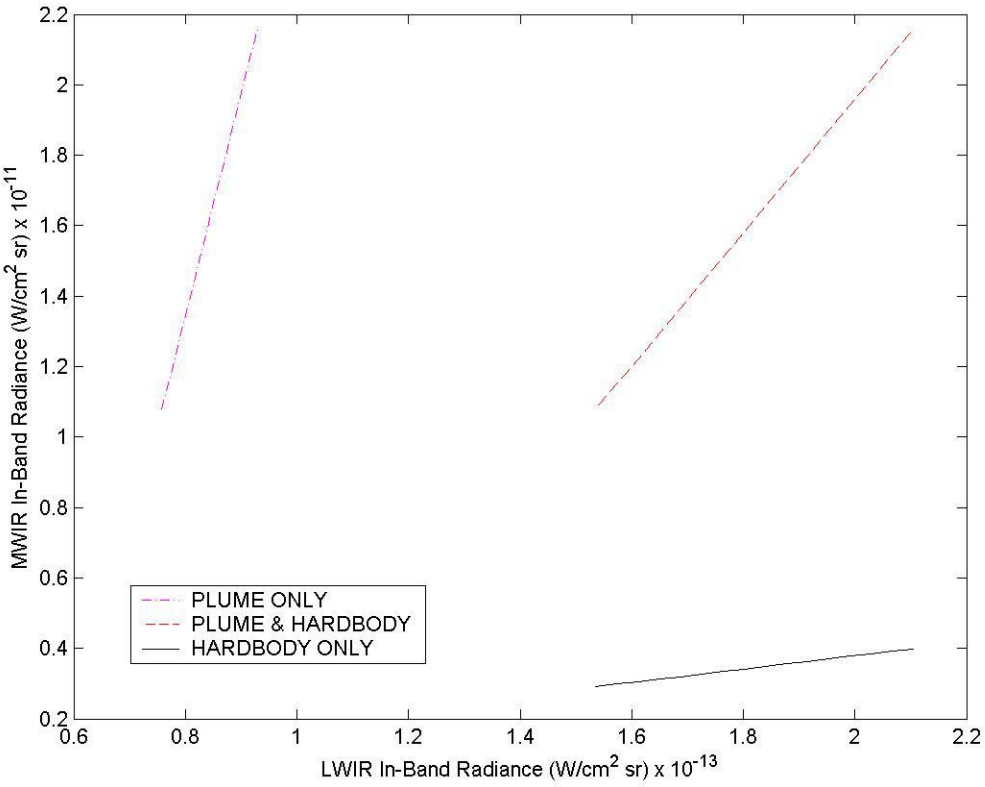

Figure 8. MWIR/LWIR Band-Ratioing.

Figure 8 shows unique lines are generated for the various target-combinations that may be in the sensor's field of view, such as only the plume at great distances, or both the plume and missile hardbody as the KV closes the target, or only the hardbody during the terminal maneuvers of the engagement.

In conjunction with band-ratioing, background subtraction is conducted to adjust the gain on each of the two image sensors, MWIR and LWIR. This will eliminate background sources of radiation such as the sky and sun to ensure that the band-ratioing calculations are only evaluated for target sources.

Initially, the target plume will produce a dominant signature in the MWIR band. The band-ratioing technique will generate values similar to those for the *plume only line* in Figure 8 and the kill vehicle will track on the power centroid of the plume. As the kill vehicle closes on the target, skin friction emissions associated with the BM hardbody will become highly visible in the LWIR band. The band-ratioing technique will generate values similar to the *hardbody only line* in Figure 8, and the kill vehicle will switch to track-

ing the leading edge of the missile hardbody. Resolution of the hardbody will permit discrimination of the optimum aimpoint on the nosecone section of the ballistic missile. This is accomplished by displacing the aimpoint from the leading edge to the specified default location.

The applicability of dual band imaging is demonstrated in Figure 9, which exhibits an Atlas V rocket, 2 minutes after liftoff, at a downrange of 35 km and an altitude of 24 km. The plume signature is saturated in both bands; however, the missile hardbody is clearly visible in the LWIR band.

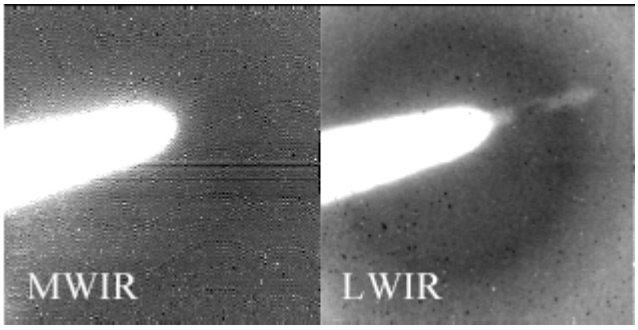

Figure 9. Dual Band IR Image of Atlas V Launch 21 August 2002 (From Ref. 13).

C. GUIDANCE

Various techniques have been proposed for strategic missile guidance including proportional navigation (PN), augmented proportional navigation, predictive guidance, and optimal control guidance (OCG) [6]. Proportional navigation is prevalent in current missile applications and considered the most effective guidance technique when accurate scientific or technical intelligence is lacking about the target missile. For example, predictive guidance requires knowledge of the threat missile's dynamics for best performance, and OCG systems are difficult to mechanize and have not been implemented to date [15]. The proportional navigation guidance law provides a basis for the simulation developed in this thesis.

1. Ideal Proportional Navigation

The definition of proportional navigation is stated as:

> The rate of change of missile heading is directly proportional to the rate of rotation of the line-of-sight (LOS) from the missile to the target [16].

The proportional navigation guidance law is mathematically expressed as

$$n_C = N' V_C \dot{\lambda} \tag{7}$$

where n_C is the commanded normal acceleration, N' is the effective navigation ratio which determines the extent of damping in the associated control system, V_C is the closing velocity between kill vehicle and target, and $\dot{\lambda}$ is the angular line-of-sight rate from kill vehicle to target ballistic missile. The effective navigation ratio is a dimensionless parameter, empirically determined to be most effective in the range of 3 to 5. An ideal representation of proportional navigation excludes system dynamics and is known as a zero-lag guidance system as shown in Figure 10.

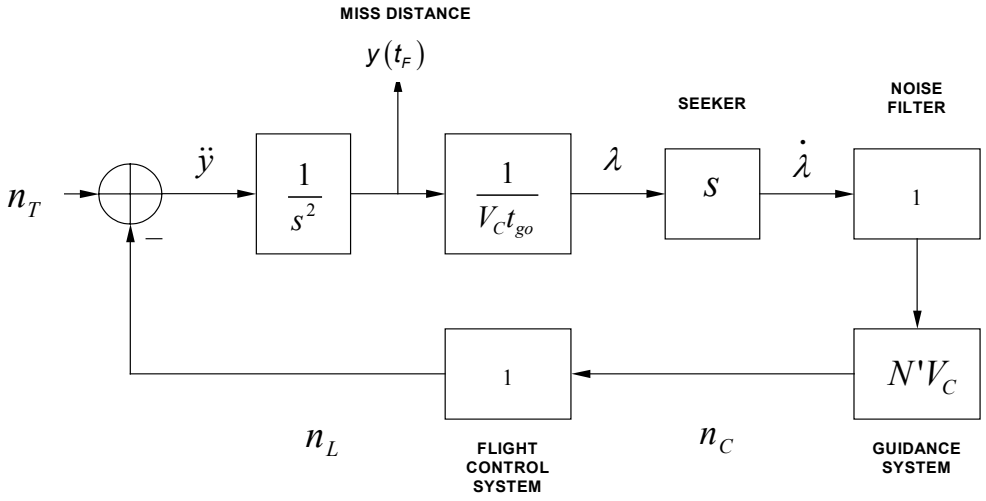

Figure 10. Ideal Representation of Proportional Navigation (After Ref. 17).

The variables displayed in Figure 8 include the achieved lateral acceleration of the kill vehicle n_L, the target normal acceleration n_T, the commanded acceleration n_C, and the relative acceleration between target and kill vehicle $\ddot{y}$ as given by

$$\ddot{y} = n_T - n_L . \tag{8}$$

The relative acceleration is transformed by double integration into relative position y, which is equal to the miss distance at the end-of-flight time t_F. The time-to-go until intercept completion is given by

$$t_{go} = t_F - t \tag{9}$$

where t is the current time. Division of the relative position by the range-to-target $\left(V_C t_{go}\right)$ produces the geometric line-of-sight angle λ as follows

$$\lambda = \frac{y}{V_C t_{go}}. \tag{10}$$

The seeker tracks the target by differentiation of λ to generate $\dot{\lambda}$. Idealized system dynamics permit unity gain representation of the noise filter. The commanded acceleration n_C as previously stated in Equation 1 is indicative of proportional navigation and provides the guidance commands to the flight control system. Lastly, the flight control system employs small rocket thrusters to maneuver the KV with respect to vertical and horizontal axes to ensure a direct hit with the optimum aimpoint on the target. The flight control system is also designated as unity gain because of the idealized representation. The achieved lateral acceleration n_L is the end result of the flight control system responding to the guidance commands.

If this ideal system were physically realizable, every engagement scenario would result in a constant-bearing course with parallel consecutive line-of-sight paths and assured destruction of the target, assuming acceleration saturation was preempted. In other words, the miss distance would always be reduced to zero at termination of the engagement. Consequently, a higher-order model of the guidance system dynamics is required to preclude an unrealistic representation of proportional navigation systems.

2. Binomial Series Representation of PN Guidance System Dynamics

A binomial series representation of the guidance system dynamics provides an effective means for modeling a more realistic proportional navigation system [17]. A representation of the system dynamics in the s domain is given by

$$\left(1+\frac{s\tau}{n}\right)^{n} = 1 + n\left(\frac{s\tau}{n}\right) + \text{H.O.T.} \tag{11}$$

where τ is the guidance system time constant, n is the system order, and H.O.T. represents higher-order terms, which have a minor effect on the model and are omitted for simplicity. A fifth-order representation, considered suitable for a preliminary analysis of kill vehicle performance, allocates five equivalent time constants as follows: one for the seeker, one for the noise filter, and three for the flight control system in Figure 11.

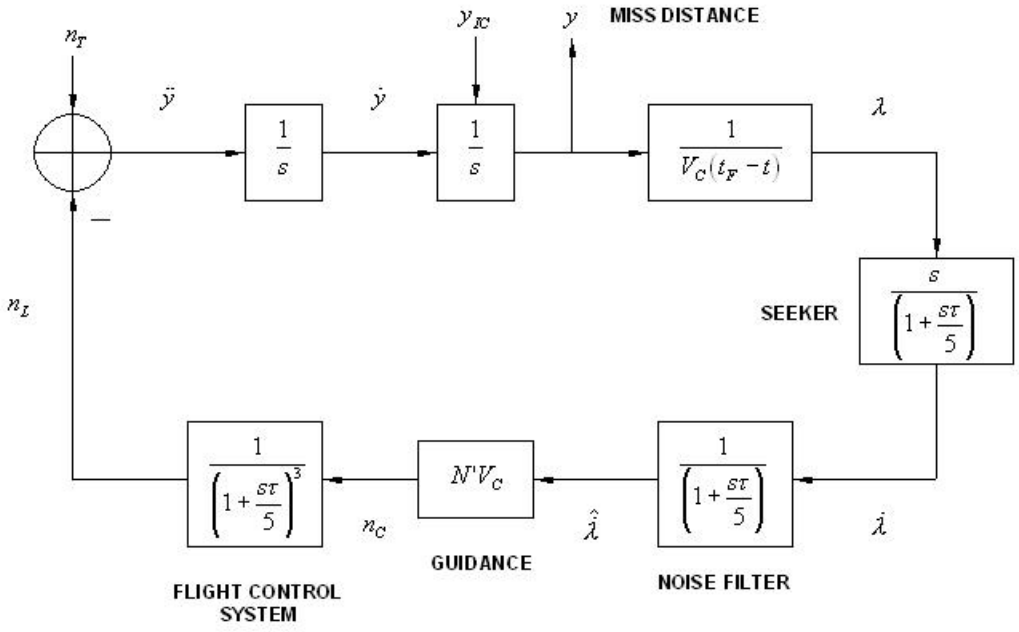

Figure 11. Fifth-Order Representation of PN Guidance System (After Ref. 18).

In this representation, the noisy line-of-sight rate must be filtered to produce a better estimate of $\dot{\lambda}$. Subsequently, the guidance commands are generated on the basis of the filtered output. In this model of PN, the response to the guidance commands is also affected by the flight control system dynamics. Also shown in Figure 11 is the parameter y_{IC}, which is used to enter the aimpoint displacement as an initial condition of the guidance simulation. The transfer function for the system shown in Figure 9 is given by

$$\frac{n_L}{\lambda} = \frac{N' V_C s}{\left(1 + \frac{s\tau}{5}\right)^5}. \tag{12}$$

The effect of system dynamics on the calculation of miss distance is made evident in Figure 12, which shows

> how the miss distance due to a 3g target maneuver varies with flight time and system order for a binomial guidance system in which the effective navigation ratio is 4 and the effective guidance system time constant is 1 s. We can see that the performance projections resulting from a single-lag guidance system model are a serious underestimate of the influence of target maneuver on miss when the flight time is not an order of magnitude greater than the guidance system time constant [17].

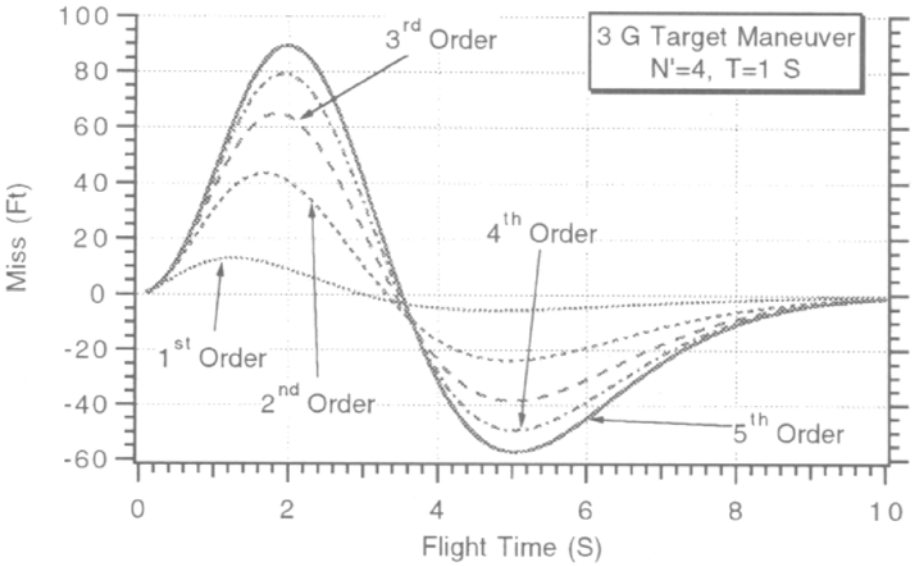

Figure 12. Comparison of System Dynamics (From Ref. 17).

It is apparent in Figure 12 that the first-order system will underestimate the amount of miss distance generated. For example, in an engagement of duration 3 seconds, the first-order system indicates a negligible miss distance, whereas the fifth-order system indicates a miss distance of 45 feet. If these engagements transpired in actuality, the kill vehicle with a first-order system would assume, just prior to termination of engagement, that it was going to hit the aimpoint and cease to make corrections. The kill

vehicle with the fifth-order system would continue to make corrections to reduce the miss distance. The negative segment of each curve indicates that the kill vehicle is below the target while the positive segment is above the target. Based on the greater accuracy provided by the fifth-order system, it was used in the ensuing simulation.

The operability of a kill vehicle for BPI is predicated on the integration of the various technologies described in this chapter. To accomplish the seemingly impossible task of hitting a bullet with a bullet, as some pundits have described this undertaking, the efficacy of the guidance and control system is paramount. The next chapter presents a simulation of the kill vehicle guidance system operating in a boost phase intercept environment. The simulation enables determination of the acceleration required by the kill vehicle and a suitable time constant for the guidance system dynamics.

THIS PAGE INTENTIONALLY LEFT BLANK

IV. SIMULATION

The simulation models the terminal maneuvers of the kill vehicle, following separation from the last stage of the intercept booster. Prior to commencement of the simulation, it is assumed that the kill vehicle has target lock-on and is tracking the ballistic missile exhaust plume via radiant emissions in the MWIR band. Until such time, the kill vehicle guides to an aimpoint at the power centroid of the target exhaust plume. As the kill vehicle closes on the target, the ballistic missile hardbody will become visible in the LWIR band. At this time, the ballistic missile warhead is resolved, and the guidance aim point shifts almost instantaneously from the plume to the warhead. This apparent target displacement occurs late in the intercept scenario and is modeled as a step input to the kill vehicle guidance system. The simulation demonstrates the affect of aimpoint displacement on miss distance and is used to determine a time constant suitable for the guidance system dynamics to reduce miss distance to a negligible amount.

It has been previously noted that a ballistic missile accelerates for the duration of boost phase; therefore, the simulation is also used to determine what acceleration capability is required by the kill vehicle to preclude saturation and ensure lethal impact with the accelerating target.

The original simulation was developed by Zarchan [17] to study the effects of an apparent target displacement that occurs when the sensor tracking point shifts from the power centroid of multiple unresolved targets to one resolved target.

A. NUMERICAL METHOD

The kill vehicle guidance system is modeled as a fifth-order binomial series representation in MATLAB. The model utilizes differential equations to represent the input/output relationships of the seeker, noise filter, and flight control system.

A second-order Runge-Kutta numerical integration method is used to solve the differential equations describing the kill vehicle guidance system [19]. The main difficulty in the numerical solution of ordinary differential equations is the solution of the first-order equation:

$$\frac{dy}{dt} = f(y,t) \tag{13}$$

with respect to the initial condition of $y = y_0$ at $t = t_0$. The Runge-Kutta technique generates approximations to the values of the solution $y(t)$ on a specified set of t values. The first step in the pointwise solution of the initial-value problem, $dy/dt = f(y,t)$ with $y(t_0) = y_0$, is to approximate the value of y at $t_1 = t_0 + \Delta t$, where Δt is the time increment. This new value of y is generated from the previous value of y plus two additional terms that are proportional to the derivative evaluated at t and at $t + \Delta t$, as given by

$$y_1 = y_0 + \frac{\Delta t}{2} f(y,t) + \frac{\Delta t}{2} f(y, t + \Delta t). \tag{14}$$

After y_1 has been generated as an approximation to $y(t_1)$ the procedure can be repeated to the desired length of t, which is time in this simulation.

B. SYSTEM DYNAMICS

The simulation incorporates a fifth-order binomial series representation of the kill vehicle guidance system components. In particular, the seeker differentiates the line-of-sight angle and is represented by the transfer function

$$\frac{\dot{\lambda}}{\lambda} = \frac{s}{\left(1 + \frac{s\tau}{5}\right)}. \tag{15}$$

The noise filter provides a smoothed estimate of the angular line-of-sight rate, designated $\hat{\dot{\lambda}}$, with the applicable transfer function stated as

$$\frac{\hat{\dot{\lambda}}}{\dot{\lambda}} = \frac{1}{\left(1 + \frac{s\tau}{5}\right)}. \tag{16}$$

Proportional navigation commands are generated on the basis of

$$\frac{n_C}{\hat{\dot{\lambda}}} = N' V_C. \tag{17}$$

Lastly, the relationship between actual and commanded acceleration of the kill vehicle is dependent on the flight control system, which is represented by the transfer function given by

$$\frac{n_L}{n_C} = \frac{1}{\left(1+\frac{s\tau}{5}\right)^3}. \tag{18}$$

The flight control system has a third-order representation to accommodate the autopilot and divert thrusters, which comprise the divert and attitude control system.

C. SYSTEM IMPLEMENTATION IN MATLAB

A schematic representation of the system components, including the variable names used in the MATLAB code is presented in Figure 13. All transfer functions identified in the previous section are implemented in code using the variable names indicated in Figure 13. This representation of the individual transfer functions permits determination of the system states by numerical integration. A description of the transformation of Equation 9 into the components of loop 1 in Figure 13 is provided in Appendix B.

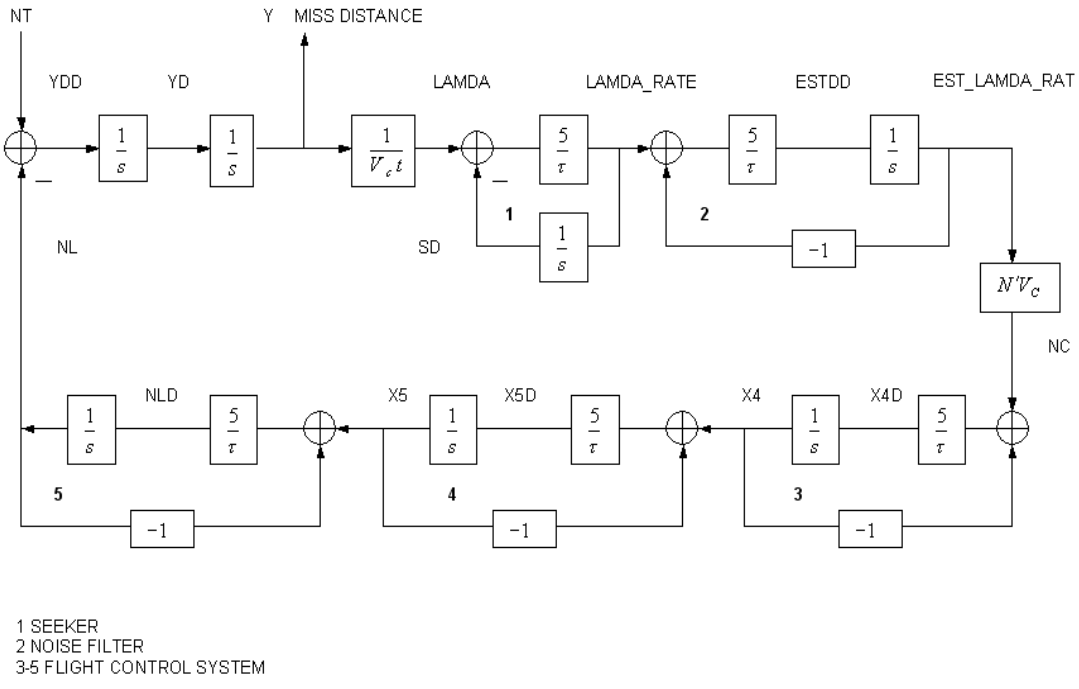

Figure 13. Simulation of Guidance System Components.

The MATLAB code representing the kill vehicle guidance system is attached in Appendix C. The simulation facilitates the analysis of the effects of various acceleration saturations and how they impacts miss distance. It is also utilized to examine how an apparent target displacement during the terminal maneuvers affects miss distance. In both cases, the data is presented in a normalized form to ensure transparent summarization. Miss distance is normalized with respect to displacement at initial condition, and the total flight time is normalized with respect to guidance system time constant. The system time constant is a critical parameter since it reflects a percentage of total time required for system response to an input signal.

1. Acceleration Saturation

An ideal guidance system employing proportional navigation will always reduce the miss distance to zero if the kill vehicle has sufficient acceleration capability. The closed form solution for acceleration n_C required by a kill vehicle with a zero lag guidance system engaging an accelerating target n_T is given by [17]

$$\frac{n_C}{n_T} = \frac{N'}{N'-2}\left[1-\left(1-\frac{t}{t_F}\right)^{N'-2}\right]. \tag{19}$$

Even for this idealized situation, a nonzero miss distance will occur if the kill vehicle-target maximum acceleration ratio defined by

$$\mu = \frac{n_{C\max}}{n_{T\max}} \tag{20}$$

does not satisfy the inequality

$$\mu \geq \frac{N'}{N'-2}. \tag{21}$$

In Figure 14, the acceleration ratio n_C/n_T is plotted for the three common values of N', with respect to normalized time t/t_F. It is apparent that maximum acceleration is required at the end of the engagement, and this maximum requirement decreases as N' is

increased. For $N' =$ 3, 4, and 5, the value of μ is equivalent to 3, 2, and 1.67, respectively.

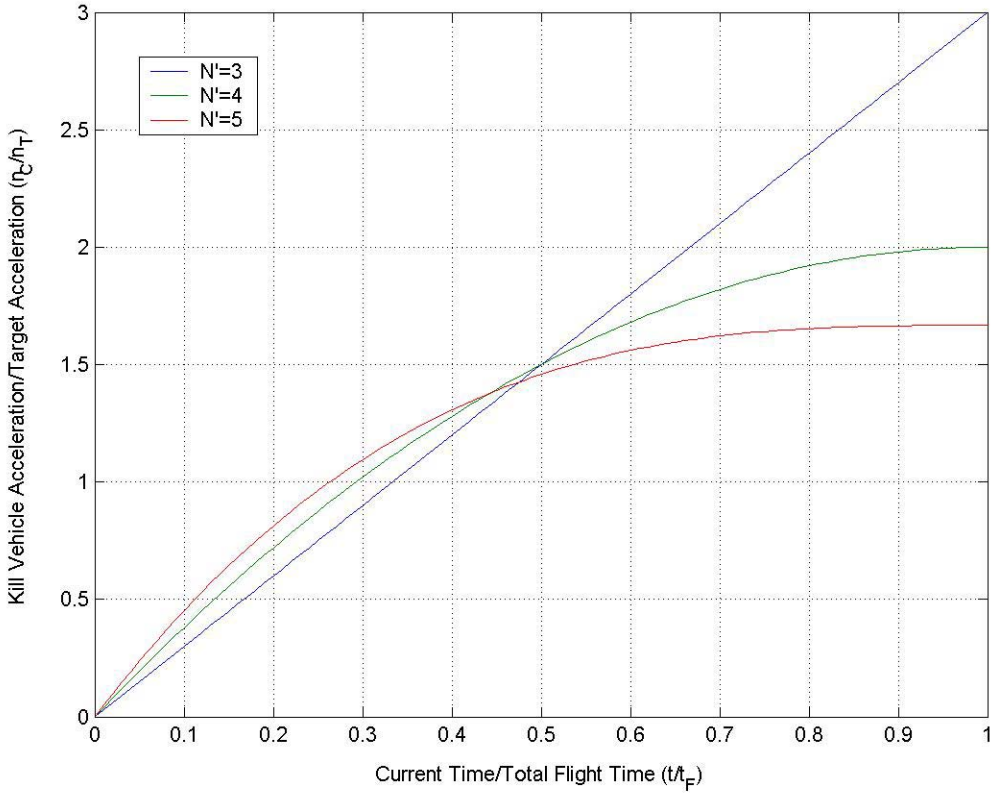

Figure 14. Normalized KV Acceleration for Zero Lag System.

This closed form solution is not applicable to the more realistic guidance system examined herein; therefore, the simulation is used to determine the value of μ and, hence, the KV acceleration capability required to intercept an intermediate range ballistic missile, which has an average acceleration of 3g, a burn time of 90 seconds, and a range of 1000 kilometers [1]. These values are representative of the North Korean No-Dong intermediate range ballistic missile, which is based on the older technology Scud missile. The simulation may easily be altered to accommodate other threat missiles. Engagement outcomes are plotted for a range of n_C/n_T values from 2 to infinity, with respect to miss distance versus total flight time remaining after target resolution. The target lateral acceleration is perceived as a maneuver by the KV guidance system; therefore, miss distance is normalized with respect to KV-target separation distance attributed to the ma-

neuver. The simulation is run separately for the three effective navigation ratios of $N' = 3,\ 4$, and 5. Graphs are generated for each run and displayed in Figures 15, 16, and 17, respectively. In each case, plots for infinite acceleration capability are shown for comparison purposes only. The run time t_F represents the total simulated engagement time, which commences at target resolution in this model, and is designated as Total Flight Time in the following graphs. The simulation run time t_F is not to be construed as the total flight time of a missile from boost phase to terminal phase. The simulation also incorporates a time-loop, which progressively increases t_F to examine scenarios of increasing duration and thereby determine the effect of guidance time on miss distance.

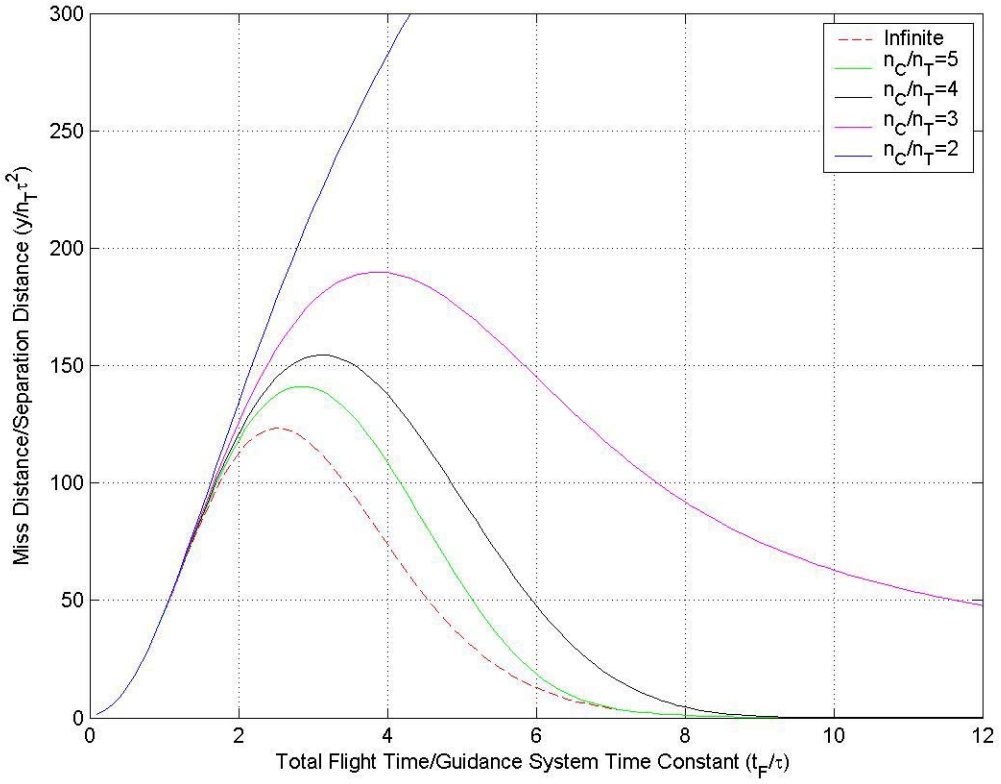

Figure 15. Normalized Miss Distance Due To Target Acceleration for $N' = 3$.

Figure 15 displays the simulation results for a kill vehicle guidance system utilizing $N' = 3$. It is clear that an acceleration ratio of 2 or less will fail to reduce the miss distance to zero. Increasing the acceleration ratio to 3 also fails to minimize the miss dis-

tance within a useful time frame. The minimum acceleration ratio, which effectively reduces miss distance to zero, is $n_C/n_T = 4$. This indicates that a kill vehicle with acceleration 4 times greater than the target will have the capability to reduce the miss distance to zero for flight times greater than nine times the guidance system time constant. In the case where the target average acceleration is 3g, the KV acceleration required would be 12g.

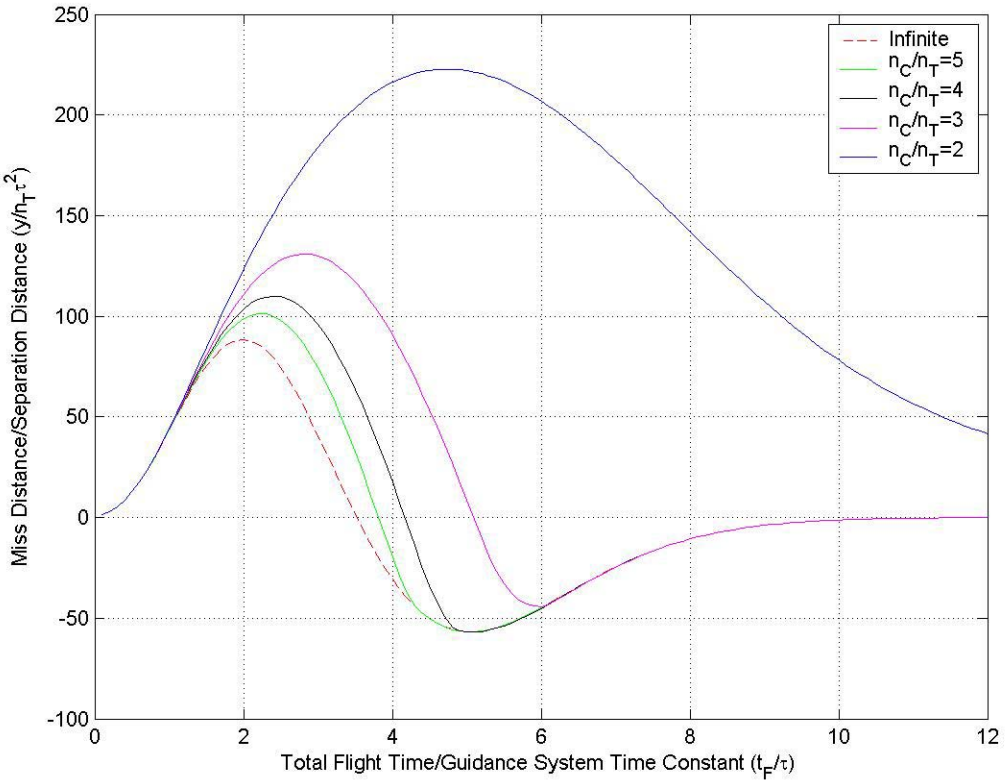

Figure 16. Normalized Miss Distance Due To Target Acceleration for $N' = 4$.

Figure 16 shows the results for $N' = 4$, where the miss is approximately zero for flight times that are ten times greater than the guidance system time constant, and the saturation limit is at least 3 times the target acceleration. Lastly, Figure 17 shows the results for $N' = 5$, where the miss is approximately zero for flight times that are twelve times greater than the guidance system time constant, and the saturation limit is at least 2 times the target acceleration. The results of these simulations are summarized in Table 2. It is apparent that increasing the effective navigation ratio N' results in decreasing the

acceleration requirement for the kill vehicle; conversely, the total flight time required for intercept increases.

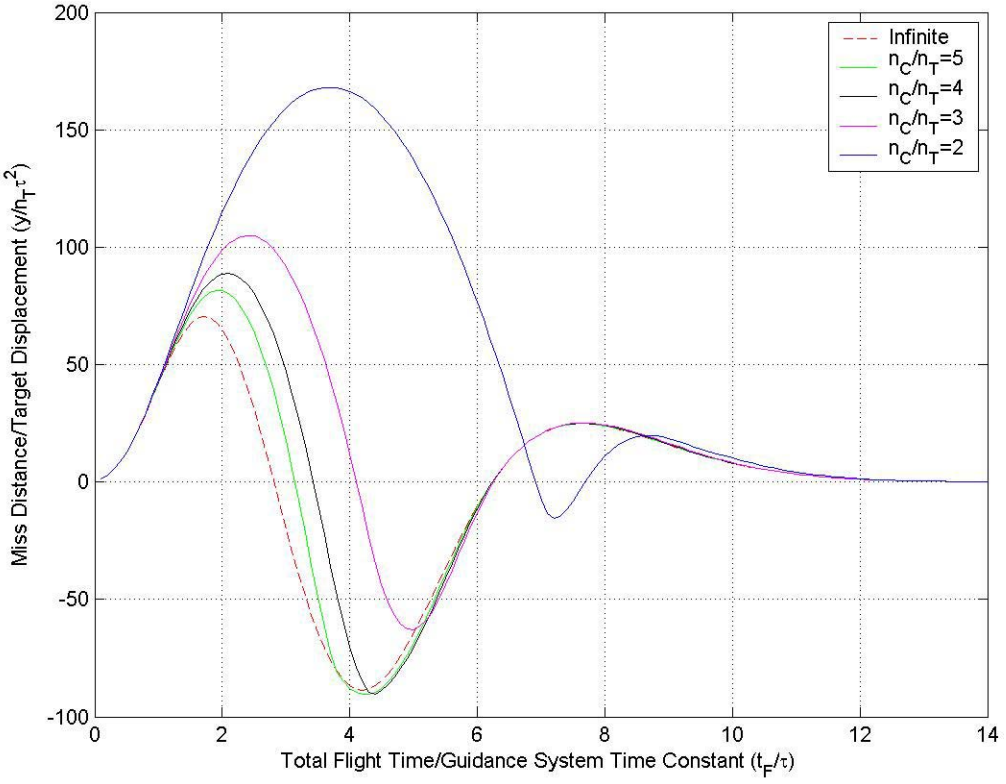

Figure 17. Normalized Miss Distance Due To Target Acceleration for $N' = 5$.

Effective Navigation Ratio (N')	**Total Flight Time After Target Resolution (t_F)**	**KV Acceleration Requirement (n_C)**
3	9τ	$4n_T$
4	10τ	$3n_T$
5	12τ	$2n_T$

Table 2. KV Acceleration Requirements for Zero Miss Distance.

2. Aimpoint Displacement

An ideal proportional navigation system that experiences an aimpoint displacement during its terminal maneuvers will recover and ultimately hit the sweet spot, assuming adequate acceleration capability. A closed form solution of the KV acceleration capability required to impact a target after a step displacement of the aimpoint is given by [17]

$$n_C = \frac{N'\left(1 - t/t_F\right)^{N'-2} y_{IC}}{t_F^2} \tag{22}$$

where y_{IC} represents initial displacement of the target aimpoint. Equation 22 states that the acceleration requirement is greatest at the time when aimpoint displacement occurs, and that n_C is proportional to the amount of displacement y_{IC}. It can also be deduced that miss distance is zero at $t = t_F$. The normalized acceleration provided by the closed-form solution is plotted for the three common values of N' in Figure 18.

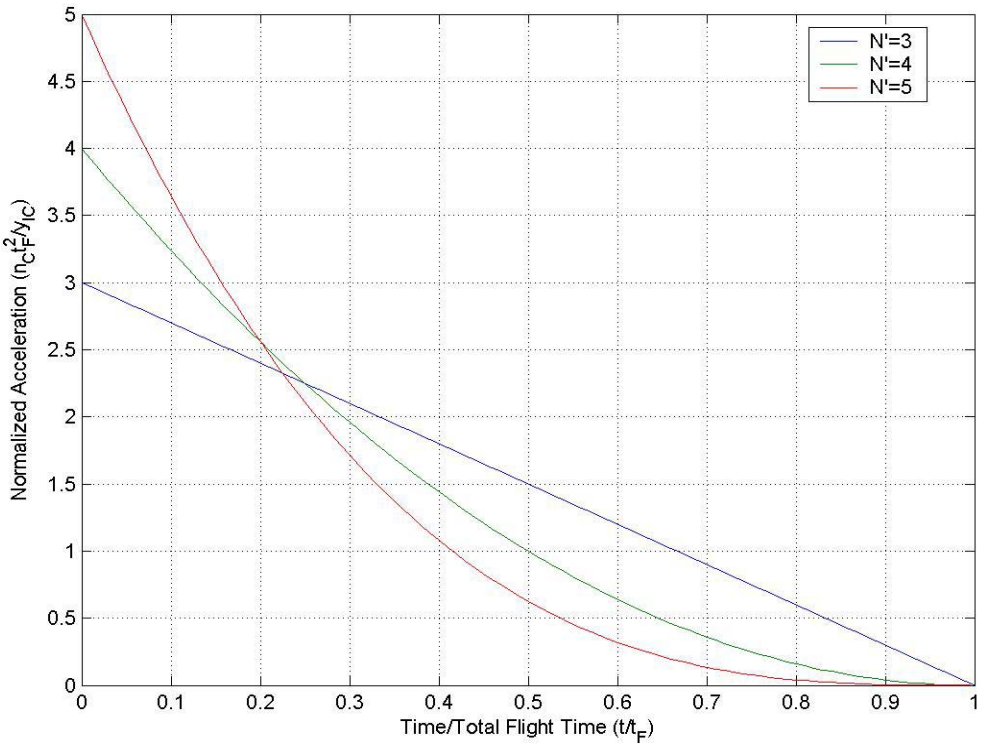

Figure 18. Normalized Acceleration Due To Aimpoint Shift For Ideal System.

An approximate demarcation point can be seen in Figure 18 at $t/t_F \approx 0.25$; up to that time, increasing the effective navigation ratio from 3 to 4 or 5 resulted in guidance commands necessitating greater acceleration capability to execute, and subsequent to that time the acceleration requirement decreased for increasing N'.

A closed-form solution is not available for determining the miss distance triggered by aimpoint displacement in a fifth-order system, as used in this simulation. Therefore, KV-target engagement outcomes are generated on the basis of the dimensionless parameter (DP) given by

$$DP = \frac{0.5 n_{C\max} \tau^2}{y_{IC}}. \tag{23}$$

The parameter DP is directly proportional to the maximum acceleration capability of the kill vehicle $n_{C\max}$. Figures 19, 20, and 21 display normalized miss distance curves attributed to an aimpoint displacement equivalent to the initial condition y_{IC}. Systems with effective navigation ratios of $N' = 3$, 4, and 5 are considered separately. In each case, graphs are generated with DP equivalent to 0.1, 0.2, 0.5, 1, and infinity for comparison. As in the previous simulation, each increment of t_F represents a separate KV-target engagement time frame resulting in a specific miss distance. For example, at $t_F = 0$ there would be zero homing time remaining after the aimpoint displacement; consequently, the kill vehicle would miss the sweet spot by an amount equivalent to the total aimpoint displacement or $y = y_{IC}$.

Examination of Figures 19, 20, and 21 reveals that acceleration capability is inversely proportional to the total flight time or number of system time constants required to minimize the miss distance to zero. In other words, as the value of DP is increased, the number of time constants required is decreased. However, kill vehicles with large acceleration capability are prone to increased overshoot of the target and may reach an unwanted miss distance that is greater than the original aimpoint displacement as evidenced in Figure 21 for $DP = 1$ at approximately $t_F = 4.5\tau$. Conversely, there is a probability for kill vehicles with less acceleration capability to incur a smaller miss distance

than the highly energetic kill vehicles. In the boost phase intercept scenario, zero miss distance is ideally required to ensure complete destruction of target payload.

Figure 19 shows the results for $N' = 3$, where the miss distance is approximately zero for flight times that are eight times greater than the guidance system time constant. Figure 20 shows the results for $N' = 4$, where the miss distance is approximately zero for flight times that are nine times greater than the guidance system time constant. Lastly, Figure 21 shows the results for $N' = 5$, where the miss distance is approximately zero for flight times that are ten times greater than the guidance system time constant. The results of this simulation are summarized in Table 3. Use of a time constant less than or equivalent to one-tenth the flight time remaining after aimpoint displacement will ensure the effectiveness of KV guidance system response for all three values of N'.

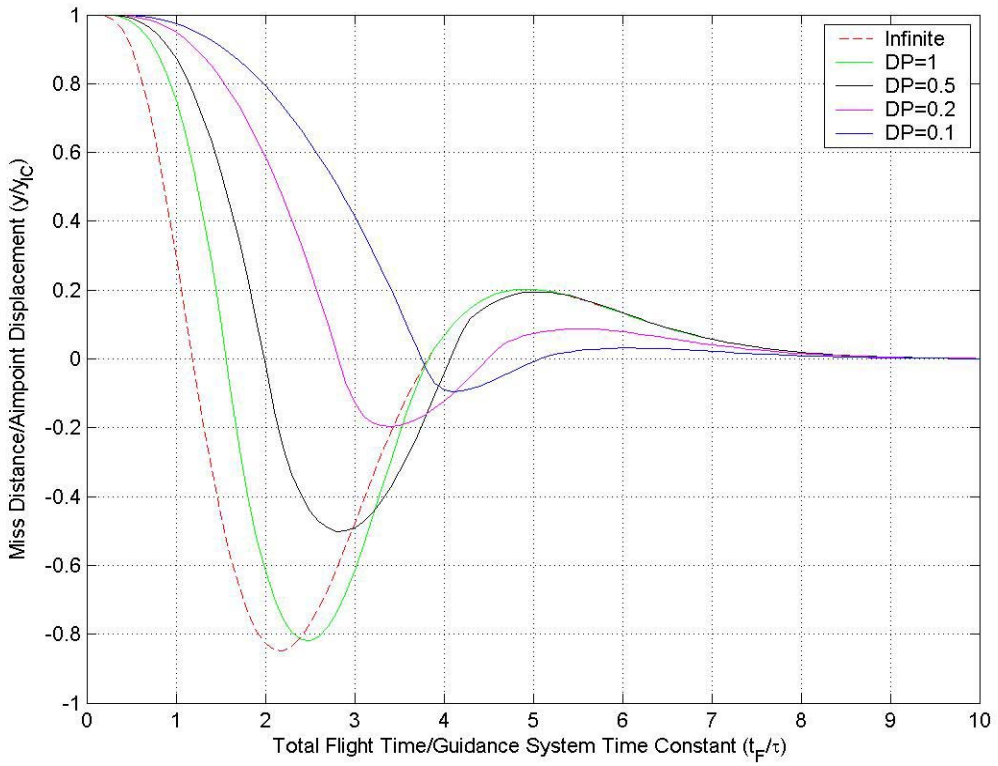

Figure 19. Normalized Miss Distance Due to Aimpoint Displacement for $N' = 3$.

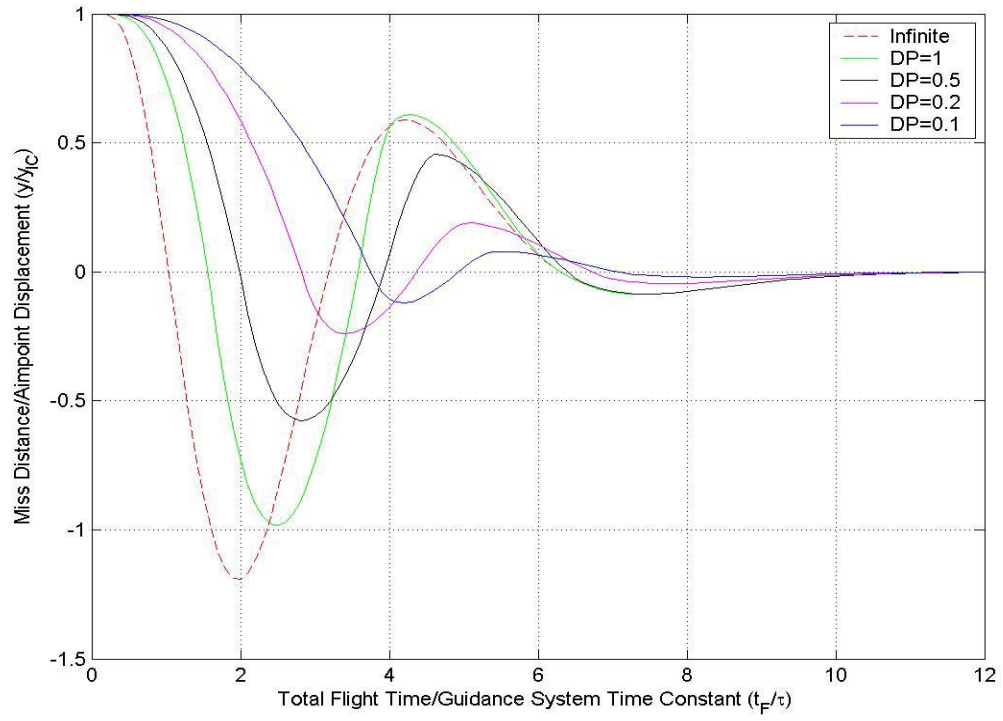

Figure 20. Normalized Miss Distance Due to Aimpoint Displacement for $N' = 4$.

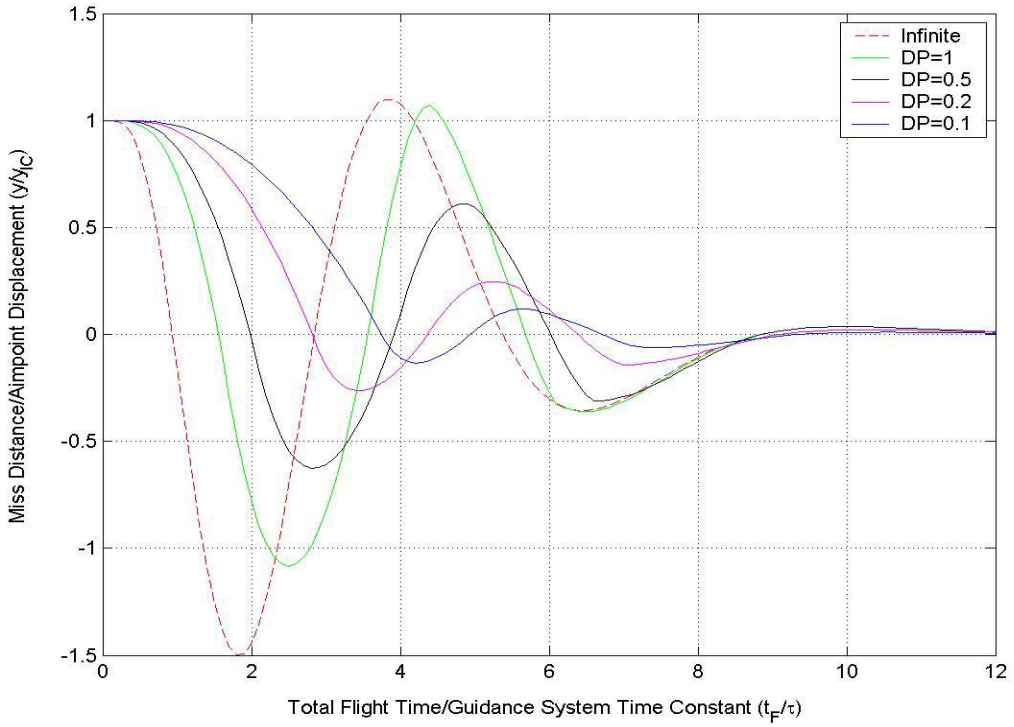

Figure 21. Normalized Miss Distance Due to Aimpoint Displacement for $N' = 5$.

Effective Navigation Ratio (N')	Total Flight Time (t_F) Remaining After Aimpoint Displacement
3	8τ
4	9τ
5	10τ

Table 3. Aimpoint Displacement Results.

The graphs displayed in Figures 19, 20, and 21 may be used to determine the amount of miss distance incurred for any displacement of the aimpoint when the maximum acceleration capability and guidance system time constant of a kill vehicle are specified. In our case, the KV acceleration requirements generated in the previous section are used in conjunction with the prerequisite for zero miss distance to determine a suitable time constant for the KV guidance system. Equation 23 is employed to calculate the time constants for $DP = 0.1$ and $DP = 1.0$ curves, listed in Table 4. The original aimpoint displacement is assumed to be equivalent to 60 feet, based on the length of the No-Dong missile plus an offset for the location of the power centroid of the plume.

DP	$4n_T$	$3n_T$	$2n_T$
0.1	0.18	0.20	0.25
1.0	0.56	0.64	0.79

Table 4. KV Guidance System Time Constants (Seconds).

To minimize the probability of overshoot, the $DP = 0.1$ curve is most applicable; secondly, to reduce the intercept time, it is necessary to use the guidance system with $N' = 3$, which requires a maximum acceleration capability of $n_C = 4n_T$. On the basis of these considerations, it is recommended that a time constant of 0.18 seconds be utilized.

Use of $\tau = 0.18$ seconds in conjunction with $t_F = 10\tau$ seconds enables the kill vehicle to reduce the miss distance to zero for an aimpoint displacement occurring up to 1.8 seconds prior to termination of the engagement.

The simulation facilitated the analysis of acceleration saturation and aimpoint displacement in a proportional navigation guidance system. Minimum requirements for the kill vehicle acceleration capability and guidance system time constant were determined to ensure a negligible miss distance at termination of engagement. The results are summarized in the concluding chapter.

V. CONCLUSION

Boost phase interception of ballistic missiles is constrained by the dual requirements of minimizing interception time to preempt deployment of submunitions or multiple reentry vehicles and reducing miss distance to within a few centimeters of the warhead sweet spot to ensure complete destruction of target payload.

The simulation implements proportional navigation commands, in conjunction with a fifth-order binomial series representation of the system dynamics, to assess the impact of acceleration saturation on miss distance. The simulation was also employed to assess the influence of aimpoint displacement on miss distance during the terminal maneuvers of the engagement. The target characteristics utilized were that of a No-Dong intermediate range ballistic missile.

The analysis of acceleration saturation revealed that increasing the effective navigation ratio N' results in decreasing the acceleration requirement for the kill vehicle to attain zero miss distance. Conversely, decreasing N' reduces the total flight time required for interception. Since time is the critical factor for boost phase interception of ballistic missiles, it is recommended that a guidance system with $N' = 3$ be implemented for the kill vehicle guidance system. This results in a 12g lateral acceleration requirement for the kill vehicle to completely destroy a No-Dong missile.

The analysis of aimpoint displacement confirmed that the acceleration requirement is inversely proportional to the flight time necessary to minimize the miss distance to zero. Unfortunately, kill vehicles with large acceleration capability are prone to increased overshoot of the target and may reach an unwanted miss distance that is greater than the original aimpoint displacement. The optimized time constant for the simulated guidance system was determined to be 0.18 seconds or one-tenth the flight time remaining after aimpoint displacement.

Recommendations for future research include determination of the following parametrics:

- Distance from which the onboard sensor's optics can identify the target payload;

- Fuel capacity required onboard the kill vehicle to sustain the divert rocket thrusters; and
- Maximum velocity required to perform divert maneuvers.

APPENDIX A. ALPHA KV-MODEL

A listing of the MATLAB commands used to implement the ALPHA-KV model is provided in this appendix.

```
%-----------------------------------------------------------------------------------------------
LT=0.9;         %Target Payload Length (m)
DT=0.6;         %Target Payload Diameter (m)
DS=0.08;        %Target Submunition Diameter (m)
rhot=1.5;       %Density of Target  (g/cm^3)
rhokv=1.0;      %Density of Kill Vehicle    (g/cm^3)
BHN=25;         %Target Brinell Hardness Number
co=9.5e4;       %Sound Speed of Target
NT=3;           %Number of Submunition Tiers
epsilon=0.03;  %Required Overlap Distance of Crater into Last Tier
alpha=3.54e-10;
Lc=(LT*((NT-1)/NT))+epsilon;    %Required Crater Depth
%Minimum Radius to Overlap All Submunitions
Ro=sqrt((Lc-0.5*LT)^2+(0.5*DT-DS)^2);
Rm=0.0:0.1:0.3;
vc=pi*Lc*(Ro+Rm)^2;
V=1.5:0.05:6;
for rm=1:length(Rm)
for v=1:length(V)
Lkv(v)=Lc*sqrt(rhot/rhokv);    %KV Length (m)
m(rm,v)=(2*pi*(Lc*Ro^2+Lc*Rm(rm)*(2*Ro+Rm(rm))))*0.1/(alpha*(V(v)*100
0)^2);
Dkv(rm,v)=100*sqrt(4*m(rm,v)*0.001/(pi*rhokv*Lkv(v)));
E(rm)=pi*Lc*(Ro^2+Rm(rm)*(2*Ro+Rm(rm)))*0.1/alpha;
end
end
plot(V,m')
grid
legend('R_m = 0','R_m = 10cm','R_m = 20cm','R_m = 30cm')
title(['Optimal Kill Vehicle Mass vs Relative Velocity'])
ylabel('Minimum KV Mass (kg)')
xlabel('Impact Velocity (km/s)')
%
figure(2)
plot(V,Dkv',V,100*Lkv,'k--')
legend('R_m = 0','R_m = 10cm','R_m = 20cm','R_m = 30cm','KV Length')
title(['Optimal Kill Vehicle Diameter vs Relative Velocity'])
ylabel('KV Diameter (cm)')
xlabel('Impact Velocity (km/s)')
grid
```

```
%
figure(3)
plot(Rm*100,E/1e6)
grid
%title(['Minimum Kinetic Energy for Optimized KV'])
ylabel('Required Kinetic Energy (MJ)')
xlabel('Aimpoint Offset (cm)')
```

APPENDIX B. TRANSFER FUNCTION DERIVATION

The individual transfer functions shown in Figure 11 are transformed into the loop components of Figure 13, to facilitate determination of the system states via numerical integration. The seeker block is examined here and is representative of all the other transfer function blocks. For convenience Figure 22 shows the equivalence of components.

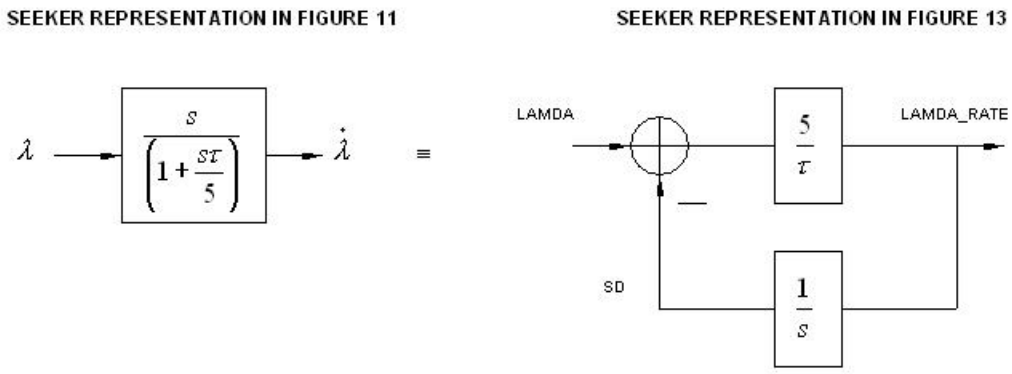

Figure 22. Transfer Function Representation.

The variable definitions for the above components are as follows:

- λ in Figure 11 is defined as LAMDA in Figure 13 and in the simulation;
- $\dot{\lambda}$ in Figure 11 is defined as LAMDA_RATE in Figure 13 and in the simulation;
- s in Figures 11 and 13 is the Laplace operator;
- SD in Figure 13 is an internal state of the seeker; and
- τ in Figures 11 and 13 is defined as TAU in the simulation.

The MATLAB code representing the seeker output is determined from the right-hand diagram in Figure 22, as

$$\text{LAMDA\_RATE} = \frac{5}{\text{TAU}}\left(\text{LAMDA} - \text{SD}\right). \tag{24}$$

To prove Equation 24 is directly related to the seeker transfer function shown in the left-hand diagram in Figure 22, note that

$$\frac{\text{SD}}{\text{LAMDA\_RATE}} = \frac{1}{s} \tag{25}$$

and substitute Equation 25 into 24, as follows

$$\text{LAMDA\_RATE} = \frac{5}{\text{TAU}}\left(\text{LAMDA} - \frac{\text{LAMDA\_RATE}}{s}\right). \tag{26}$$

$$\text{LAMDA\_RATE}*\text{TAU} = 5*\text{LAMDA} - 5*\frac{\text{LAMDA\_RATE}}{s} \tag{27}$$

$$\text{LAMDA\_RATE}\left(\text{TAU} + \frac{5}{s}\right) = 5*\text{LAMDA} \tag{28}$$

$$\frac{\text{LAMDA\_RATE}}{\text{LAMDA}} = \frac{5}{\left(\text{TAU} + \frac{5}{s}\right)} \tag{29}$$

$$\frac{\text{LAMDA\_RATE}}{\text{LAMDA}} = \frac{5}{\left(\frac{s*\text{TAU}+5}{s}\right)} \tag{30}$$

$$\frac{\text{LAMDA\_RATE}}{\text{LAMDA}} = \frac{5s}{s*\text{TAU}+5} \tag{31}$$

$$\frac{\text{LAMDA\_RATE}}{\text{LAMDA}} = \frac{s}{\left(1 + \frac{s*\text{TAU}}{5}\right)} \tag{32}$$

Equation 32 may be re-written with the symbols utilized in the left-hand diagram of Figure 22 as

$$\frac{\dot{\lambda}}{\lambda} = \frac{s}{\left(1 + \frac{s\tau}{5}\right)}, \tag{33}$$

which is the original transfer function.

THIS PAGE INTENTIONALLY LEFT BLANK

APPENDIX C. GUIDANCE SYSTEM SIMULATION

A listing of the MATLAB commands used to implement the fifth-order proportional navigation guidance simulation is provided in this appendix.

```
%Variable Definitions---------------------------------------------------------------------
%NT                     Target Acceleration
%YDD                    Relative Acceleration
%YD                     Relative Velocity
%Y                      Miss Distance
%LAMDA                  Geometric LOS
%LAMDA_RATE             Geometric LOS Rate
%SD                     Seeker Internal State
%ESTDD                  Filter Internal State
%EST_LAMDA_RAT          Filter Estimate Geometric LOS Rate
%NC                     Commanded Acceleration
%X4D                    FCS Autopilot Internal State
%X4                     FCS Autopilot Output
%X5D                    FCS Divert Internal State
%X5                     FCS Divert Output
%NLD                    FCS Internal State
%NL                     Achieved Acceleration
%Begin Simulation-------------------------------------------------------------------------
VC=32808.               %Closing Velocity
G=32.2                  %Acceleration due to gravity
NT=3*G                  %Target Lateral Acceleration
DISPLACE=1.             %Aimpoint Displacement
TAU=1.                  %Kill Vehicle Guidance System Time Constant
NPRIME=4.               %Effective Navigation Ratio
NCLIM=10e10             %Acceleration Saturation Infinite Limit for KV
n=0                     %Pass Number
for TF=0.1:0.1:12       %Outer Loop for Generating Total Flight Time
Y=DISPLACE              %Initial Condition Displacement
YD=0.                   %Enter Iteration Process Velocity
NL=0.                   %Enter Iteration Process Acceleration
SD=0.                   %Enter Iteration Process LOS Angle
EST_LAMDA_RATE=0.       %Enter Iteration Process
X5=0.                   %Enter Iteration Process
T=0.                    %Begin Iteration Process at Time = 0
DELTA=.01               %Increment Length for R-K Numerical Integration
while T<=(TF-1e-5)      %Run Iteration Until TGO Less Than/Equal 1e-5 s
YOLD=Y                  %Miss Distance
YDOLD=YD                %Miss Distance Derivative
NLOLD=NL                %Acceleration Achieved by Kill Vehicle
SDOLD=SD                %Output from Seeker Integration
```

```
EST_LAMDA_RATE_OLD=EST_LAMDA_RATE       %Estimate LOS Rate
X4OLD=X4                    %State 4 within Flight Control System
X5OLD=X5                    %State 5 within Flight Control System
STEP=1
FLAG=0
while STEP<=1
if FLAG==1                  %Conduct Iteration at Time T
STEP=2
Y=Y+DELTA*YD                %Displacement at Time T
YD=YD+DELTA*YDD             %Derivative of Position at Time T
NL=NL+DELTA*NLD             %Achieved Acceleration at Time T
EST_LAMDA_RATE=EST_LAMDA_RATE+DELTA*ESTDD
SD=SD+DELTA*LAMDA_RATE
X4=X4+DELTA*X4D
X5=X5+DELTA*X5D
T=T+DELTA                   %Increment Time
end
%Conduct Iteration at Time T+DELTA-----------------------------------------------
TGO=TF-T+0.00001                    %Time To Go
LAMDA=Y/(VC*TGO)                    %Measured Geometric LOS Angle
LAMDA_RATE=5.0*(LAMDA-SD)/TAU       %Seeker Output LOS Rate

%Filter Internal Estimated Geometric LOS Rate
ESTDD=5.0*(LAMDA_RATE-EST_LAMDA_RATE)/TAU

%Commanded Acceleration from PN Law
NC=NPRIME*VC*EST_LAMDA_RATE

if NC>NCLIM
NC=NCLIM                    %Acceleration Limit of KV
end
if NC<-NCLIM
NC=-NCLIM                   %Acceleration Limit of KV
end
X4D=5.0*(NC-X4)/TAU         %Flight Control System
X5D=5.0*(X4-X5)/TAU         %Flight Control System
NLD=5.0*(X5-NL)/TAU         %Achieved Acceleration of KV
YDD=NT-NL                   %Relative Acceleration
FLAG=1
end
FLAG=0
Y=0.5*(YOLD+Y+DELTA*YD)                     %Runge-Kutta Integration
YD=0.5*(YDOLD+YD+DELTA*YDD)                 %Runge-Kutta Integration
NL=0.5*(NLOLD+NL+DELTA*NLD)                 %Runge-Kutta Integration
SD=0.5*(SDOLD+SD+DELTA*LAMDA_RATE)          %Runge-Kutta Integration
```

```
EST_LAMDA_RATE=0.5*(EST_LAMDA_RATE_OLD+EST_LAMDA_RATE
+DELTA*ESTDD)                                   %Runge-Kutta Integration
X4=0.5*(X4OLD+X4+DELTA*X4D);                    %Runge-Kutta Integration
X5=0.5*(X5OLD+X5+DELTA*X5D);                    %Runge-Kutta Integration
end
n=n+1                                %Increment Simulation Pass Number
ArrayTF(n)=TF
ArrayY(n)=Y
end
figure
plot(ArrayTF,ArrayY,'r--')
grid
xlabel('Flight Time (Sec)')
ylabel('Miss (Ft)')
clc
output=[ArrayTF',ArrayY'];
save datfil.txt output  -ascii
disp 'simulation finished'
```

THIS PAGE INTENTIONALLY LEFT BLANK

LIST OF REFERENCES

1. Secretary of Defense, Memorandum: Missile Defense Program Direction, Washington, DC, January 2, 2002.
2. Peter J. Mantle, *The Missile Defense Equation: Factors for Decision Making*, pp. 81-92, American Institute of Aeronautics and Astronautics, Reston, VA, 2004.
3. http://raytheonmissiledefense.com/phases/ Accessed 05/04.
4. American Physical Society Study Group, "Boost-Phase Intercept Systems for National Missile Defense," pp. 261-263, (unpublished), Washington, DC, July 15, 2003.
5. Mark Hewish, "Back in the melting pot," Jane's International Defense Review, pp. 1-8, March 1, 2002.
6. Ben-Zion Naveh and Azriel Lorber, *Theater Ballistic Missile Defense*, Vol. 192, pp. 71-73 and pp. 221-241, American Institute of Aeronautics and Astronautics, Reston, VA, 2001.
7. Duncan Lennox, "Ballistic Missile Defense," Jane's Strategic Weapon Systems 40, p. 4, November 27, 2003.
8. Richard M. Lloyd, *Physics of Direct Hit and Near Miss Warhead Technology*, Vol. 194, pp. 31-81, American Institute of Aeronautics and Astronautics, Reston, VA, 2001.
9. M.R. McHenry, M.A. Levin, and D.L. Orphal, "Estimating Optimum Hit-to-Kill Vehicle Configurations for Lethality Against Submunition Payloads," AIAA 98-0831, pp. 1-4, 1998.
10. A. Tate, "Long Rod Penetration Models-Part II Extensions to the Hydrodynamic Theory of Penetration," Journal of Mechanical Science, Volume 28, Number 9, pp. 599-612, 1986

11. George P. Sutton and Oscar Biblarz, *Rocket Propulsion Elements*, Seventh Edition, pp. 639-652, John Wiley & Sons, New York, 2001.

12. Michael H. Miklaski and Joel D. Babbitt, "A Methodology for Developing Timing Constraints for the Ballistic Missile Defense System," Master's Thesis, Naval Postgraduate School, Monterey, CA, December 2003.

13. Arnold Goldberg, "Dual-Band Infrared Imaging of Tactical and Strategic Targets," presented at the 23rd Army Science Conference, Orlando, FL, December 2002.

14. Michael C. Dudzik, Editor, *The Infrared & Electro-Optical Handbook, Vol. 4*, pp. 302-303, SPIE Optical Engineering Press, Bellingham, WA, 1996.

15. N.A. Shneydor, *Missile Guidance and Pursuit Kinematics, Dynamics and Control*, pp. 202-205, Horwood Publishing Limited, Chichester, UK, 1998.

16. D. Curtis Schleher, *Introduction to Electronic Warfare*, p. 353, Artech House, Norwood, MA, 1986.

17. Paul Zarchan, *Tactical and Strategic Missile Guidance Fourth Edition*, Vol. 199, pp. 95-118 and pp. 407-431, American Institute of Aeronautics and Astronautics, Reston, VA, 2002.

18. F. Bardanis, P.E. Pace, and M. Tummala, "Kill Vehicle Effectiveness for Boost Phase Interception of Ballistic Missiles," to be presented at the International Conference on Computing, Communications and Control Technologies, CCCT 04, Austin, TX, August 2004.

19. John R. Tooley, *Numerical Methods in Engineering Practice*, pp. 424-428, Holt Rinehart and Winston, New York, 1986.

INITIAL DISTRIBUTION LIST

1. Defense Technical Information Center
   Ft. Belvoir, VA

2. Dudley Knox Library
   Naval Postgraduate School
   Monterey, CA

3. Dr. Phillip E. Pace
   Electrical and Computer Engineering Department
   Naval Postgraduate School
   Monterey, CA

4. Dr. Murali Tummala
   Electrical and Computer Engineering Department
   Naval Postgraduate School
   Monterey, CA

5. Dr. Bret Michael
   Computer Science Department
   Naval Postgraduate School
   Monterey, CA

6. Dr. Man Tak Shing
   Computer Science Department
   Naval Postgraduate School
   Monterey, CA

7. Mr. Dale Scott Caffall
   Missile Defense Agency
   Washington, DC

8. Mr. L. Lamoyne Taylor
   Raytheon
   Tucson, AZ

9. Mr. Elfriede S. Borst
   Analytical Graphics Inc
   Malvern, PA